

Study of Aldehydes, Co and characterization of particles resulting from oil contamination of
aircraft bleed air

by

Shahin Nayyeri Amiri

B.Sc., University of Tabriz, 2000

M.Sc., University of Tabriz, 2003

M.Phil. University of Tabriz, 2006

M.Sc., Kansas State University, 2010

Ph.D., Kansas State University, 2011

AN ABSTRACT OF A DISSERTATION

submitted in partial fulfillment of the requirements for the degree

DOCTOR OF PHILOSOPHY

Department of Mechanical and Nuclear Engineering

College of Engineering

KANSAS STATE UNIVERSITY

Manhattan, Kansas

2018

Abstract

Contamination of aircraft bleed air with engine oil and/or hydraulic fluid results in a “fume event” in the aircraft cabin. Exposure to contaminated bleed air may have acute and/or chronic adverse health effects based on the intensity of various chemicals which are released during such a fume event. ASHRAE Standard 161, Air Quality within Commercial Aircraft, includes a requirement for bleed air sensors to detect contamination from lubricating oil. One potential approach to meeting this requirement is through particle detection. In the research reported here, the end goal is to provide data needed to develop an automated detection apparatus for contaminated bleed air through oil particle detection. Consequently, the type and concentration of different chemicals as well as the number and size distribution of particles were determined for bleed air with different rates of contamination under various turbine engine operating conditions. Multiple fume events were simulated by using a four-part experimental program to develop a detailed characterization of particles that result when bleed air is contaminated with lubricating oil. Test results show that oil contamination in the compressor will result in a fog of very fine droplets in the bleed air under most operating conditions. With moderately high contamination rates at elevated power levels (high bleed air temperature) the concentration distribution and particle size does not vary much with power (temperature) and generally depends on the rate of contamination. Moreover, at elevated power levels, the peak particle concentration takes place in the range of 50 to 70 nanometers and the bulk of the particles form at less than 150 nanometers. At very low contamination rates very ultrafine particles can be generated in the size of 10 nanometers or less. As a result, detection is needed for a range of sizes ranging from about 100 nanometers to 10 nanometers.

Study of Aldehydes, Co and characterization of particles resulting from oil contamination of
aircraft bleed air

by

Shahin Nayyeri Amiri

B.SC., UNIVERSITY OF TABRIZ, 2000

M.SC., UNIVERSITY OF TABRIZ, 2003

M.PHIL, UNIVERSITY OF TABRIZ, 2006

M.SC., KANSAS STATE UNIVERSITY, 2010

PH.D., KANSAS STATE UNIVERSITY, 2011

A DISSERTATION

submitted in partial fulfillment of the requirements for the degree

DOCTOR OF PHILOSOPHY

Department of Civil Engineering

College of Engineering

KANSAS STATE UNIVERSITY

Manhattan, Kansas

2018

Approved by:

Major Professor

Dr. Byron Jones

Copyright

SHAHIN NAYYERI AMIRI

2018

Abstract

Contamination of aircraft bleed air with engine oil and/or hydraulic fluid results in a “fume event” in the aircraft cabin. Exposure to contaminated bleed air may have acute and/or chronic adverse health effects based on the intensity of various chemicals which are released during such a fume event. ASHRAE Standard 161, Air Quality within Commercial Aircraft, includes a requirement for bleed air sensors to detect contamination from lubricating oil. One potential approach to meeting this requirement is through particle detection. In the research reported here, the end goal is to provide data needed to develop an automated detection apparatus for contaminated bleed air through oil particle detection. Consequently, the type and concentration of different chemicals as well as the number and size distribution of particles were determined for bleed air with different rates of contamination under various turbine engine operating conditions. Multiple fume events were simulated by using a four-part experimental program to develop a detailed characterization of particles that result when bleed air is contaminated with lubricating oil. Test results show that oil contamination in the compressor will result in a fog of very fine droplets in the bleed air under most operating conditions. With moderately high contamination rates at elevated power levels (high bleed air temperature) the concentration distribution and particle size does not vary much with power (temperature) and generally depends on the rate of contamination. Moreover, at elevated power levels, the peak particle concentration takes place in the range of 50 to 70 nanometers and the bulk of the particles form at less than 150 nanometers. At very low contamination rates very ultrafine particles can be generated in the size of 10 nanometers or less. As a result, detection is needed for a range of sizes ranging from about 100 nanometers to 10 nanometers.

Table of Contents

List of Figures.....	viii
List of Tables.....	vii
Acknowledgements.....	x
Dedication	xi
Chapter 1–Introduction.....	1
Chapter 2 –Brief description of instrumentation.....	4
2.1 Sep-pak DNPH silica and charcoal sorbent tubes.....	4
2.2 Fourier transform infrared spectroscopy (FTIR).....	5
2.3 Scanning mobility particle-sizer spectrometer.....	9
2.4 Aerodynamic particle sizer.....	11
2.5 An overview of particle measuring equipment setup for this study.....	13
Chapter 3 – Literature review.....	16
Chapter4–Study of Aldehydes, co & particulate contaminants generated in bleed air simulator...	22
4.1 Bleed air system.....	22
4.2 Bleed air simulator.....	23
4.3 Test procedure.....	24
4.4 Results and discussion.....	25
4.5 Conclusions of this study.....	36
Chapter5–Characterization of particles resulting from oil contamination of aircraft bleed air....	38
5.1 Experimental program.....	38
5.1.1 Allison 250 c18 turbine engine.....	39
5.1.2 Allison 250 c28 B turbine engine.....	42
5.1.3 Pratt and Whitney F 11/PW 2000 turbine engine.....	44
5.2 Results and discussion.....	46
5.3 Conclusions from this study.....	60
Chapter 6–Conclusions and recommendation for further research	62
References.....	65
Appendix A – Project setup pictures.....	68

List of Figures

Figure 1.1 Typical bleed air system in commercial transport aircraft.....	3
Figure 2.1 Sep-pak DNPH-silica and charcoal sorbent tubes.....	5
Figure 2.2 Fourier transform infrared (FTIS).....	8
Figure 2.3 Model 3080 electrostatic classifier.....	9
Figure 2.4 APS and SMPS setup.....	12
Figure 4.1 Main duct and sampling part of simulator.....	24
Figure 4.2 Variation of aldehyde concentration versus temperature.....	26
Figure 4.3 Variation of aldehyde concentration for different temperatures	27
Figure 4.4 Concentration of aldehydes for constant pressure at two different temperatures.....	27
Figure 4.5 Detailed mass and number of concentration data at 200 kp.....	29
Figure 4.6 Detailed mass and number of concentration data at 345 kp.....	30
Figure 4.7 Detailed mass and number of concentration data at 480 kp.....	31
Figure 4.8 Detailed mass and number of concentration data at 690 kp.....	32
Figure 4.9 Detailed concentration data at 185°C	33
Figure 4.10 Detailed concentration data at 220°C	33
Figure 4.11 Detailed concentration data at 250°C	34
Figure 4.12 Detailed concentration data at 280°C	34
Figure 4.13 Detailed concentration data at 310°C	35
Figure 5.1 Allison 250 c18 turbine engine.....	40
Figure 5.2 Schematic of Allison 250 c18 turbine engine.....	41
Figure 5.3 TDA-4B lite laskin nozzle unit.....	41
Figure 5.4 250 c28B turbine engine.....	44
Figure 5.5 Test setup for Pratt and Whitney F11/PW 200.....	45
Figure 5.6 Distribution number of particles respect to c18 engine.....	47
Figure 5.7 Distribution number of particles mass respect to c18 engine.....	48
Figure 5.8 Distribution number of particles respect to c28 B engine.....	49
Figure 5.9 Distribution number of particles mass respect to c28 B engine.....	49
Figure 5.10 The decay trend of number of particles for c 28 engine.....	50

Figure 5.11 The decay trend of number of particles mass for c 28 engine.....50
Figure 5.12 The decay trend of number of particles for c 28 B engine.....51
Figure 5.13 The decay trend of number of particles mass for c 28 B engine.....51
Figure 5.14 Distribution of particles respect to air force c 17 aircraft.....57
Figure 5.15 Distribution of particles mass respect to air force c 17 aircraft.....58

List of Tables

Table 2.1 Gas library for FTIR measurement calibration.....	7
Table 4.1 Temperatures and pressures values.....	25
Table 4.2 Concentration for different temperatures, pressures measured by FTIR.....	28

Acknowledgements

First and most, all praises be to source of all goodness who is the Lord of the universe, the most gracious, and the most merciful.

I would like to express my deepest gratitude to my advisor, Prof. Byron Jones, for the immeasurable amount of support, guidance and valuable advice throughout the research. His continued support led me to the realization of this work.

I note with appreciation the guidance, support and encouragement of the Examining Committee Members, namely Prof. Mohammad Hosni, Prof. Steven Eckels, Prof. Hayder Rasheed, and Prof. Amy Betz.

I would like to thank Prof. Asad Esmaily, Prof. Hani Melhem, Prof. Donald Fenton, and Prof. Terry Beck for their contributions to my education at the Kansas State University.

This research was funded, in part, by the U.S. Federal Aviation Administration (FAA) Office of Aerospace Medicine through the National Air Transportation Center of Excellence for Research in the Intermodal Transport Environment. This support is gratefully acknowledged. Publication of this information does not imply FAA endorsement of the results or any conclusions drawn. The cooperation and support of NASA and Air Force throughout the VIPR experiments and the inclusion of the bleed air experiments in the VIPR program are greatly appreciated. The bleed air portion of the VIPR test platform was designed and constructed by Boeing and Boeing led the VIPR bleed air research team. The oil injection system for the VIPR engine was designed, built, and operated by Auburn University.

Dedication

This dissertation is dedicated to *my mother*, who has always given me the encouragement to complete all tasks that I undertake and continuously supports me whenever I face any difficulty in my life as well as for her love and sacrifice. To *my sister, Yasaman*, who has always inspired and helped me and to *my niece, Selena*.

CHAPTER 1 - Introduction and Purpose of this Research

Air travelers breathe a blend of recirculated cabin air and outside air known as bleed air that has been compressed by the aircraft engines. Occasionally, engine oil leaks into bleed air, resulting in various chemical contaminants entering the aircraft cabin. Determining the chemicals produced and the oil particle size distribution when bleed air becomes contaminated with engine oil is very important to evaluate potential adverse health effects and to design a sensing system to detect bleed air contamination in real time. Figure 1.1 shows a bleed air duct used in most of commercial transport aircraft manufactured by Airbus Industries.

ASHRAE Standard 161, Air Quality within Commercial Aircraft, includes a requirement for bleed air sensors to detect contamination from lubricating oil. One potential approach to meeting this requirement is through particle detection.

Accordingly, in the research reported here, the final goal is to provide data needed to develop an automated detection apparatus for contaminated bleed air through oil particle detection. For that purpose, a four-part experimental program was conducted to assess the nature of contaminants that result from oil contamination of bleed air. These experiments addressed the chemical nature and the particulate (droplet) nature of the contamination that eventually ends up in the bleed air. There were multiple objectives for the projects including quantification of the chemical exposure that results, identification of chemical tracers for detection, and characterization of the particulates that result. The first part of the program utilized a bleed air simulator. A reciprocating compressor followed by a heated tube was used to create controlled temperature and pressure conditions representative of bleed air from an aircraft engine. Aerosolized lubricating oil was injected into the airflow upstream of the compressor and the particulate characteristics were measured downstream of the heated tube. The second and third parts of the program used turbine shaft

engines mounted in a test stand and connected to a dynamometer for controlled loading. Aerosolized oil was mixed into the inlet air and the resulting particle characteristics in the bleed air were measured. The compressor for the second part utilized both axial and centrifugal compression stages while the compressor for the third part utilized a single centrifugal stage. The fourth part of the program utilized an engine on an US Air Force C-17 military transport aircraft. Oil was injected into the first stage of the compressor and the bleed air from the engine was diverted to a test platform where it was cooled and sampled. Particulate size distributions and concentrations were measured with aerodynamic particle sizing and scanning mobility particle sizing. Collectively, these instruments could measure concentrations and size distributions for particles ranging from 10 nanometers to 20 microns. Sep-Pak DNPH-Silica and Charcoal Sorbent Tubes in conjunction with mass spectrometry as well as Fourier transform infrared spectroscopy (FTIR) were used for identifying different types of chemicals.



Figure 1.1: Typical bleed air system in commercial transport aircraft [1]

CHAPTER 2 - Brief descriptions of instrumentation

In this research three different devices or measurement systems were used to determine different chemicals and characterize the aerosols. A description of the instrumentation and measurements employed follows.

2.1 Sep-Pak DNPH-Silica and Charcoal Sorbent Tubes

DNPH (2,4-Dinitrophenylhydrazine-coated) silica cartridges analyzed by HPLC/UV and charcoal sorbent tubes extracted with carbon disulfide/acetone and analyzed by GC/MS were used for collecting and detecting aldehydes and organic vapors, respectively. They were attached to air sampling pumps operated at a flow rate of 1 liter/min for 20 min for sample collection. Sorbent tubes are sealed glass tubes, with generally 2 sections of adsorbent material. The ends of the sorbent tube are broken off and inserted into a tube holder which is then connected to a personal sampling pump. DNPH-cartridges are usually used for analyzing formaldehyde, other aldehydes and ketones in air and charcoal tubes were evaluated primarily for aromatic hydrocarbons, alcohols, and long chained aldehydes. A library search of all major peaks was done to identify the major by-products formed.



Figure 2.1: Sep-Pak DNPH-Silica and Charcoal Sorbent Tubes

2.2 Fourier Transform Infrared Spectroscopy (FTIR)

Fourier transform infrared spectroscopy (FTIR) is another method for identifying chemicals that are either organic or inorganic. FTIR spectroscopy is a technique based on the determination of the interaction between infrared radiation and a sample which can be solid, liquid or gaseous. It measures the infrared frequencies at which the different samples absorb as well as the intensities of absorption. The absorption frequency spectrum is helpful for the detection of the sample's chemical structure because of the fact that chemical functional groups are responsible for the absorption of radiation at diverse frequencies. The concentration of a component can be inferred from the intensity of the absorption. The FTIR spectrum generally is a two-dimensional plot in which the axes are shown by intensity and frequency of sample absorption. The FTIR technique presents the potential for the simultaneous, non-destructive, and real-time measurement

of multiple gas phase compounds in complex blends. All compounds show a characteristic absorption in the IR spectral region and, based on this property, they can be analyzed both quantitatively and qualitatively. This works best for single gases or simple mixtures and cannot be used for all compounds, only those with functional groups that have reasonably strong absorption in bands in the IR range, and it is often hard to distinguish between compounds with similar functional groups. It can detect carbon monoxide and formaldehyde with good accuracy, provided the levels are high enough. FTIR's advantages over other measurement techniques include direct sampling of raw exhaust, measurement of many compounds with one analyzer and highly-stable calibrations. In this study, FTIR model Nicolet 6700 was used to measure carbon monoxide and formaldehyde, and it was set to 0.5 cm^{-1} resolution because, at lower resolutions, water's absorbance bands may create interference problems which affect the detection limits. The detection limits for both gases was 2 ppm. The water vapor concentrations in the bleed air were much higher than for the chemicals of interest which tends to interfere with their measurement with the FTIR. The strong interference of water vapor in the sample line stream is overcome by detecting chemical substances in narrow bands of the IR spectrum where water absorption is very weak. The transfer line between the engine and the FTIR should be heated to prevent condensation. A heated particulate trap is required to stop soot particles from coating onto the gas cell mirrors. In addition, a vacuum pump is required to pull the exhaust through the sampling system. Table 2.1 lists the library gas which was used for measurement calibration.

Table 2.1: Gas library for FTIR measurement calibration.

Compound	Concentration Range (ppm)
Carbon monoxide	20-400
Carbon dioxide	1660-15000
Nitrogen monoxide	60-1100
Nitrogen dioxide	6-100
Dinitrogen monoxide	20-400
Methane	200-3000
Formaldehyde	10-100
Ethylene	50-400
Butane	25-200
Propane	50-200
Ethane	50-400
Ammonia	50-400
Benzene	5- 200



Figure 2.2: Fourier Transform Infrared (FTIR), Model: Nicolet 6700 setup at NGML

2.3 Scanning Mobility Particle-Sizer Spectrometer

A scanning mobility particle-sizer spectrometer (SMPS) consists of an electrostatic classifier followed by a condensation particle counter. In this study, the TSI model 3080 electrostatic classifier was used. It includes the Model 3081 Long Differential Mobility Analyzer (Figure 2.3)



Figure 2.3: Model 3080 Electrostatic Classifier with Model 3081 Long DMA

It works based on the physical principle that the ability of a particle to traverse an electric field (electrical mobility) is fundamentally related to particle size and no size calibration is necessary (first principle measurement). In a differential mobility analyzer (DMA), an electric field is created and the airborne particles drift in the DMA according to their electrical mobility. Particle size is then calculated from the mobility distribution. Sizing limitations of surface techniques include low sample sizes (non-representative), image edge definition problems, 3D to 2D image distortion, and operator bias. The manufacturer specified uncertainty is approximately equal to 3 – 3.5% for size and $\pm 10\%$ for concentration. The Electrostatic Classifier selects aerosol particles of uniform size from a polydisperse source, resulting in a highly monodisperse aerosol. The Long DMA offers classification in the range from 10 to 1000 nanometers in diameter. The Electrostatic Classifier separates particles by size for high-resolution measurements of particle size distribution. When used in TSI Scanning Mobility Particle Sizer (SMPS) spectrometers, for example, monodisperse aerosol exiting the Electrostatic Classifier passes to a Condensation Particle Counter (CPC), which measures particle number concentration. By scanning quickly through a portion of the size range from 2 to 1000 nanometers (size range varies by SMPS configuration), the SMPS measures the size distribution of the aerosol precisely. The electrostatic classifier was used with a TSI model 3775 CPC, which detects airborne particles down to 4 nm. It gives accurate measurements over a wide concentration range from 0 to 10^7 particles/cm³. In this apparatus, an aerosol sample is passed continuously through a heated saturator where butanol is vaporized and diffuses into the aerosol sample stream. Together, the aerosol sample and butanol vapor pass into a condenser where the butanol vapor becomes supersaturated and ready to condense. Particles present in the sample stream serve as condensation nuclei. Once condensation begins, particles quickly grow into larger droplets and pass through an optical detector where they

are counted easily. The manufacturer specified uncertainty for the CPC is $\pm 10\%$ of the reading to concentration less than 5×10^4 particles/cm³ and it drops to $\pm 20\%$ of the reading for 5×10^4 particles/cm³- 10^7 particles/cm³.

2.4 Aerodynamic Particle Sizer

The TSI Aerodynamic Particle Sizer (APS-Model 3321) is a high-performance, general-purpose particle spectrometer that measures both aerodynamic diameter and light -scattering intensity. It measures particles in the range from 0.5 to 20 micrometers using a time-of-flight technique that measures aerodynamic diameter in real time. Because time-of-flight aerodynamic sizing accounts for particle shape and is unaffected by index of refraction or Mie scattering, it is superior to sizing by light scattering. Aerodynamic diameter is the most important size parameter because it determines a particle's airborne behavior. The Model 3321 is specifically engineered to perform aerodynamic size measurements in real time using low particle accelerations. The particle stream is kept centered by a sheath flow as they pass through focused laser beams. The larger particles lag more in the air stream than smaller ones and thus the flight time between the particles is altered. Light is scattered as the particles pass through the two beams and exit the equipment. From this scattered light the equipment is able to pick up the time of flight information and convert it into a calibrated aerodynamic particle size. These particles are then binned into 52 channels on a logarithmic scale. Particles between 0.3 and 0.5 micrometers are able to be detected, but the statistical chance that the detection is false rises rapidly with decreasing particle size as the extinction coefficient rises exponentially. Furthermore, the monotonic response curve of the time-of-flight measurement ensures high-resolution sizing over the entire particle size range.



Figure 2.4: APS and SMPS setup during test running

2.5 An Overview of Particle Measuring Equipment Setup for This Study

The particles in the bleed air were evaluated using a scanning mobility particle sizing spectrometer (SMPS) and an aerodynamic particle sizer spectrometer (APS) as indicated in Figure 2.4. The SMPS has a nominal size range of 10 – 1000 nanometers (0.01 – 1.0 μm) and the APS had a nominal size range of 0.5 μm to 20 μm . The two instrument systems combined provide a wide range of coverage with respect to particle size. The SMPS consisted of a TSI 3080 electrostatic classifier equipped with a TSI 3081 long diffusion mobility analyzer (DMA) connected to a TSI 3775 butanol-based condensation particle counter (CPC). The APS was a TSI 3221 aerodynamic particle sizer equipped with a TSI 3302A diluter. Aerosol instrument manager software supplied by the manufacturer was used to operate all of the particle measuring equipment and for data reduction. Detailed information about the operation of these systems is provided by TSI (2009, 2012).

There are two key temperature limitations associated with the particle measuring equipment. The CPC saturator is controlled to 39°C and the CPC optics are maintained at 40°C to ensure there is no butanol condensation on the optics. In order to maintain proper temperature control, the operating environment and the sample air need to be below 39°C. The CPC cools the air to 14°C to drive the condensation and particle growth. In order to ensure that there is no water condensation on the particles, the dew point of the sample air needs to be below 14°C. If the air dew point is above this value, the air stream needs to be dried upstream of the measuring instruments. The VIPR measurements were conducted in the Mojave Desert at Edwards Air Force Base and, consequently, dew point was never a concern due to the dry atmosphere. VIPR III operational upper temperature limits not associated with the SMPS were similar and no data were

collected outside of these limits. Additionally, cooling air was directed into the instrument bays to offset solar heating of the equipment platform. For the test stand measurements, scheduling of experiments was more flexible and experiments could be run when limits were not exceeded.

The stated accuracy of the APS with respect to size is $+0.03\mu\text{m}$ and is $+20\%$ with respect to concentration. The state accuracy of the SMPS as configured for these experiments is $+3.5\%$ with respect to size and $+20\%$ with respect to concentration. Characterization of aerosols can be distorted by several factors associated with the measurement process in addition to inaccuracies associate with the instruments. For all three engines, there is a tortuous path between the engine and the point where the sample stream for the particles is extracted and measured. Certainly, particles could be lost along this flow path. The goal of this study, however, is not to determine precisely the nature of the particles as they come out of the engine. Rather, the goal is to determine the nature of the particles that would be sampled for detection of oil contamination in the bleed air on an aircraft. As a minimum, the bleed air would pass through at least one pressure regulator and the pre-cooler before it would be sampled on an aircraft. Thus, the experimental apparatuses used in these experiments are reasonably representative of an actual aircraft. The main concern is the distortion that would occur between the sample point and the instrument. Roth [18] conducted a detailed assessment of particle loss and distribution distortion. This assessment shows that any losses or distortion occurring between the sample point and the instruments is small compared to the accuracy limits of the instruments.

Given the high-speed rotating machinery associated with the engine compressors and the tortuous path involve in cooling the bleed air in the pre-coolers, few micron and larger particles were expected. The APS was included to verify that important phenomena regarding these larger particles were not missed. As expected, few, if any, useful data in this size range were collected

and only SMPS data are reported here. The SMPS data can be presented in several ways. The instrument is typically operated so there are 64 size bins distributed equally by the logarithm of the diameter. The data are then presented in terms of number concentration divided by the logarithm of the bin size, $dN/d\log(D_p)$, and in terms of the mass concentration divided by the logarithm of the bin size, $dm/d\log(D_p)$. The units for number concentration are particles per cm^3 and the units for mass concentration are $\mu\text{g}/\text{m}^3$.

CHAPTER 3 - A Brief History and Literature Review

Air travelers (passengers and flight crews) are increasingly concerned about the air quality of aircraft cabins. Air travelers breathe a blend of recirculated cabin air and outside air that has been compressed by the aircraft's engine known as bleed air. Occasionally, engine oil leaks into bleed air, resulting in various chemical contaminants entering the aircraft cabin. Contaminated bleed air has been known to be potentially toxic to passengers and crew since 1953 [2]. Identifying the potential for fume events and determining their frequency is very important. Few reliable studies have been done to determine the frequency of fume events [3]. Shehadi et al. [3] reviewed and analyze existing data on fume events. The results of their study showed that fume events have taken place in aircraft from all major aircraft manufacturers and are spread amongst all aircraft models, propulsion engine models, and APU models. However, they found some aircraft models with higher incident frequencies, up to five times the overall average. Variations in incident frequencies from airline to airline could not be determined from the database used for the study. Due to increasing concerns of air travelers and crew members about the air quality in aircraft cabins, researchers and design engineers have become increasingly interested in the study of contaminants generated when engine oil migrates into the bleed air stream [4].

According to the Winder et al. [4] study, exposure to contained bleed air do produce symptoms of toxicity. As a result, the aviation industry is coming under increasing pressure to improve its standards due to public anxiety regarding bleed air contamination.

Murawski [5] studied air contamination events for one major US airline over a two-year period. According to the findings in this study, a total of 87 fume events were reported. The research showed that the crew health, flight safety, and operational impact of exposure to

contaminated bleed air is very important. It was concluded that several of these events may have been prevented and/or their impact could have been eased with better coordination using proper crew, maintenance worker training, and protocols to screen and replace mechanical components before they reach the end of their service life. Recommendations included installing and operating suitable bleed air monitoring and cleaning equipment.

Nagda et al. [6] reviewed measured air concentrations of organic contaminants in the aircraft cabin and supply air. They compared these concentrations with those reported for buildings and other transportation modes such as buses. Their study showed that, although some differences exist between aircraft and other environments, the measured concentrations of organics are low in the aircraft. It should be noted that their measurements were during normal operations and not during fume events.

Guan et al. [7] conducted in-flight measurements during normal operation without fume incidents in 107 commercial flights from August 2010 to August 2012. They selected flights randomly and developed a sampling method using a syringe to collect air samples to obtain overall information of volatile organic compounds (VOCs) in aircraft cabins. On average, 59 different VOCs on each flight were detected, with a total of 346 VOCs in the 107 flights.

Bartl et al. [8] investigated thermal degradation of pentaerythritol derivatives which are the base component of jet engine oils. They used thermogravimetric analysis and differential thermal analysis. They heated pentaerythritol from room temperature up to 1000 °C. According to their findings, the sample starts to lose weight at roughly 275 °C and lower temperature oxidation

reaction occurs at approximately 350 °C. Finally, they concluded oxidation of any remaining oil and charred products to CO and CO₂ take place at 525 °C.

In order to investigate the thermal breakdown of jet engine oils, Van Netten et al. [9] heated two different available jet engine oils in the laboratory. They found that jet oil starts to produce smoke and to lose mass at 275 °C. They increased temperature to 525 °C to measure the release of CO, CO₂, NO₂, HCN and volatile organic compounds. They did not detect trimethyl propane phosphate (TMPP), HCN and NO₂ in these experiments. Above the heated oil they found that CO₂ generated along with CO which reached levels in excess of 100 ppm. The measured concentration was in a confined vessel and not in flowing bleed air. Based on their investigation, above 500 °C volatile compounds are produced and they are almost identical in the two different oils. These volatile compounds do not exist in the two oils. They confirmed the presence of TCPs in the bulk oils and in the vapors generated. Their observation showed solid black residue remains after heating jet engine oils. They hypothesized that some of the volatilized components and pyrolysis products could condense out of the airstream onto the interior surface of the aircraft ventilation system during a fume event and not reach the cabin.

It should be noted that bleed air temperature in typical commercial aircraft, depending on operation mode, can possess temperatures ranging from 185 °C to 310 °C [9] so oil temperatures in studies done by Bartl et al. [8] and Van Netten et al. [9] are well above the operating range of modern aircraft engines.

In a typical aircraft, depending on its operational mode, bleed air can possess various pressures and temperatures ranging from 200 to 690 kPa and 185 °C to 310 °C respectively. Mann et al. [10] analyzed the particulate size distribution and concentrations of oil particles in a bleed air simulator. They presented particle counter data of the oil droplets from simulated jet engine

bleed air. For this purpose, they used four different particle counters which, collectively, covered a range of 13nm to 20 μ m. Their tests results show a considerable increase of fine particles as the temperature is increased up to 320 °C, approximately the maximum temperatures expected during normal aircraft operation. Based on their finding, the pressure of the bleed air has much less effect on the particle-size and concentration than the temperature.

Reddall [11] wrote a paper titled “Elimination of engine bleed air contamination”. In this paper, two alternative solutions are suggested: the aircraft should be designed with an outside air compressor independent of the engines and/ or that engine bleed air should be filtered.

Lebbin [12] evaluated the flight deck and cabin fire and smoke incidents reported to the Canadian airworthiness authorities over a ten year span. The study categorized the fire and smoke related diversions to identify areas where efforts could be increased to improve safety. According to the paper, the Canadian airworthiness authorities received over 1,000 smoke and fire incidents from the years 2001 to 2010, of which, over 680 reported fire or smoke in the flight deck and cabin compartments for various makes and models of aircraft.

Supplee et al. [13] attempted to characterize the frequency of oil contamination and its impact on health and on operational costs. They concluded that, both on the ground and in flight, the outside air supplied to a cabin and flight deck by the propulsion engine or APU can be contaminated with engine oil or hydraulic fluid. Their analysis shows an average of 0.86 events per day over an 18- month period.

Day. [14] investigated the potential health-related risks because of exposure to bleed air contaminants generated during fume events. The study concluded that, without comprehensive detection and measurements of the representative hazard in the contaminated bleed air, quantification of the potential health risks associated with bleed air contaminants is not possible.

Winder et al. [15] studied crew effects from toxic exposures on aircraft. According to their study, if engine oil leaked into the bleed air and passed to aircraft cabin, aircrew and passengers may be exposed to contaminants that can affect their health and safety. Possible symptoms include discomfort, fatigue, irritation, gastrointestinal, respiratory and nervous system effects, and long-term central nervous and immunological effects.

Ross et al. [16] investigated cognitive function following exposure to contaminated air on commercial aircraft. They wanted to determine whether there is a link between exposure to contaminated air and neuropsychological impairment. For this purpose, they selected 29 pilots and according to aircraft type flown, they put them into two exposure groups. They found few differences between the groups in terms of exposure history or cognitive function.

With the continued growth of the commercial and military fleets, there has been an increase in the frequency of investigations, recommendations, and reports of ill health and compromised aviation safety related to bleed air contamination and there is a growing call to retro-fit contamination detection systems [17].

The forgoing literature review is by no means exhaustive. However an extensive literature review on this subject shows that, up to now, several academic institutions and regulatory agencies have initiated research concerning the health effects of oil contamination within bleed air. Nevertheless, there is little, if any, published information on the nature of the aerosols that are generated and the gasses that evolve when bleed air is contaminated by engine oil. This information is important both for evaluating potential health effects from and developing detection systems for oil contamination of bleed air. Since the temperature and pressure generated in an engine compressor at the bleed port varies substantially depending upon the operating conditions and the particular engine design, it is important to document how these variables impact the nature

of the aerosol and gasses evolved. No comprehensive research to illustrate the different chemicals and their concentrations nor comprehensive research to determine the size and concentration characteristics of aerosol as a function of temperature and pressure that result from bleed air contamination were found in the literature. For these reasons, the first part of this study is undertaken to use a bleed air simulator which can recreate conditions in engine compressor bleed air and which can introduce engine lubricating oil into that air to systematically examine the impact of bleed air temperature and pressure on the resulting gasses and aerosols produced. In the second part of this study the goal is to provide the database needed to develop an automated detection apparatus (sensors) for contaminated bleed air through oil particle detection. These sensors can be installed in the air supply system and could detect when contamination occurs. Developing such sensors or implementing available sensors requires knowledge about the nature of the particulates that are to be sensed. To further the development of such a database, the number of oil particles and their size distribution were determined for bleed air with different rates of contamination under various engine operating conditions. Assessment of specific detection technology or devices is not part of the work. A lubrication oil based fume event was simulated by injecting different rates of synthetic jet engine lubricating oil (Mobile Jet II) into the intake air of two different turbine engines (Allison 250 C18 and Allison 250 C28B) and then the resulting contaminated bleed air was cooled and sampled. In addition, another series of tests was conducted on a Pratt & Whitney F117-PW-100 engine on-board an Air Force C17 aircraft under nominal and simulated oil contamination conditions with oil injected into the first stage of the compressor.

CHAPTER 4 - Study of Aldehydes, CO and Particulate

Contaminants Generated in Bleed Air Simulator¹

4.1 Bleed air system

In propulsion engines, bleed air is compressed air that is taken from the compressor of a gas turbine engine before it is mixed with fuel in the combustion chamber. There are Auxiliary Power Units which also provide bleed air, but are not addressed in this paper. Bleed air is used on many aircraft systems because it is easily available, reliable, and a source of pneumatic power. In passenger aircraft, a primary use of bleed air is to provide pressurization and ventilation for the aircraft cabin by supplying air to the cabin through the environmental control system. Bleed air is also used to keep critical parts of the aircraft (such as the wing leading edges) ice-free. Typically, engines will have two bleed air extraction ports on the engine compressor, a low stage port and a high stage port. Air from the low stage compressor section is used during high power operations, while high stage air is used during descent and other low power operations. The selection of the port is automatically controlled to maintain appropriate bleed air pressures. The temperature and pressure of the air extracted from the compressor, typically, will have temperature and pressure ranges from 200 to 300°C and 345 kPa to 690 kPa respectively, depending on engine power level and other operational factors [10].

¹ Based on: Amiri, S. N., Jones, B., Mohan, K. R., Weisel, C. P., Mann, G., & Roth, J. (2016). Study of Aldehydes, Carbon Monoxide, and Particulate Contaminants Generated in Bleed-Air Simulator. *Journal of Aircraft*, 1-11.

4.2 Bleed Air Simulator

The Bleed Air Simulator (BAS) which was used in this study had three main parts:

1. Oil droplet generation section, in which compressed air and atomizing nozzles generate an oil aerosol.
2. Compressor and heater tube section, in which a reciprocating compressor and electric heaters increase the temperature and pressure of the air carrying the aerosol.
3. Main duct, which dilutes, cools, and slows the flow of the bleed air stream, simulating the duct supplying bleed air to the aircraft cabin.

The temperature of the bleed air stream through the heater tube section was controlled by varying the voltage to the heaters and measured by a type K thermocouple with $\pm 1^\circ\text{C}$ uncertainty. Pressure of the heater tube was controlled with a back pressure regulator and measured with a 0-3447 kPa pressure transducer with $\pm 0.11\%$ full scale uncertainty. Other details of this equipment were discussed at length in [9], and will not be repeated here. The only modifications to the simulator were additional instruments added to measure chemical composition as shown in Figure 4.1.

The sample line for the fourier transform infrared spectrometer (FTIR) and sample lines for 2,4-dinitrophenylhydrazine (DNPH) cartridges and sorbent tubes were pulled directly from the compressed air line as shown in Figure 4.1 to provide gaseous contaminant concentrations that were high enough to yield good measurement accuracy. The air stream for these sample lines passed through a HEPA inline filter to remove aerosols so that only gaseous constituents were measured.

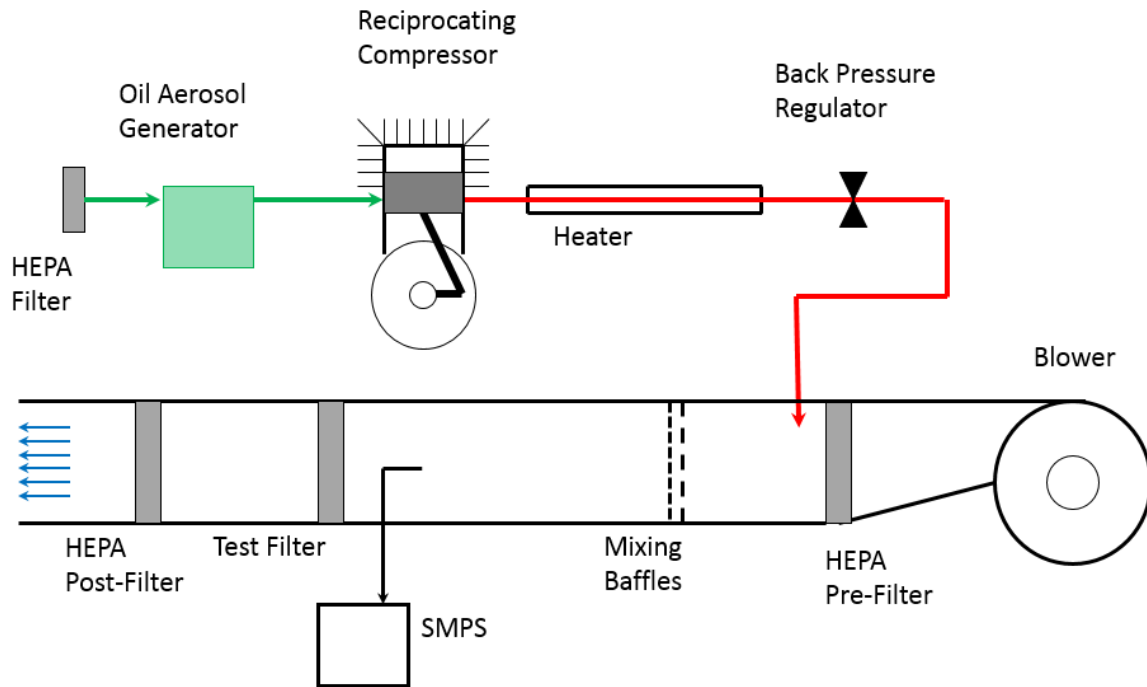


Figure 4.1: Main duct and sampling part of simulator

4.3 Test Procedure

In a typical aircraft, depending on its operational mode, bleed air can possess various pressures and temperatures ranging from 200 to 690 kPa and 185 °C to 310 °C respectively [10].

A number of measurement points within this range were collected. The test matrix is shown in Table 4.1. As evidenced from Table 4.1, there were twenty measurement points. In order to have a stable condition at each point, the system was operated for an hour and then data were recorded

for ten minutes. A detailed test procedure has been given in the Mann et al. [9] paper.

Table 4.1: Temperatures and pressures values which were used in the BAS

 Temperature (°C)	185	230	250	280	310
	200	200	200	200	200
Pressure (kPa) 	345	345	345	345	345
	480	480	480	480	480
	690	690	690	690	690

4.4 Results and Discussion

DNPH silica and charcoal tubes analysis results are summarized in Figures. 4.2 through 4.4. These graphs show that aldehyde production dramatically increased both with increasing pressure and increasing temperature in the pressure range of 200 - 480 kPa. However, at 690 kPa, increasing temperature has minimal effect. The FTIR was not able to provide accurate measurements to detect aldehydes due to their low concentrations, but it was used to measure carbon monoxide (CO) concentration (Table 4.2).

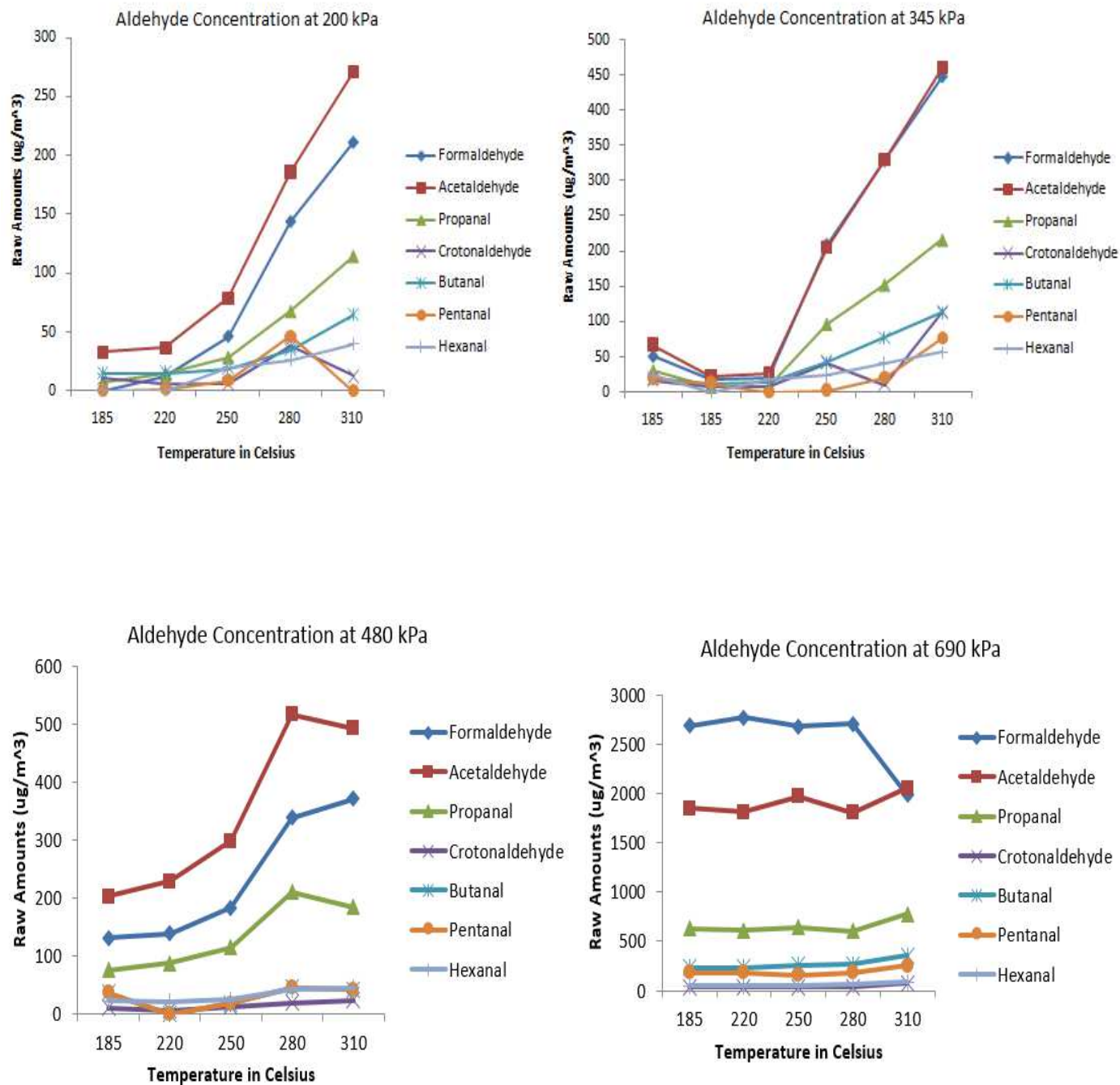


Figure 4.2: Variation of aldehyde concentration versus temperature at different pressures

Aldehyde Conc. at 310 Deg Celsius

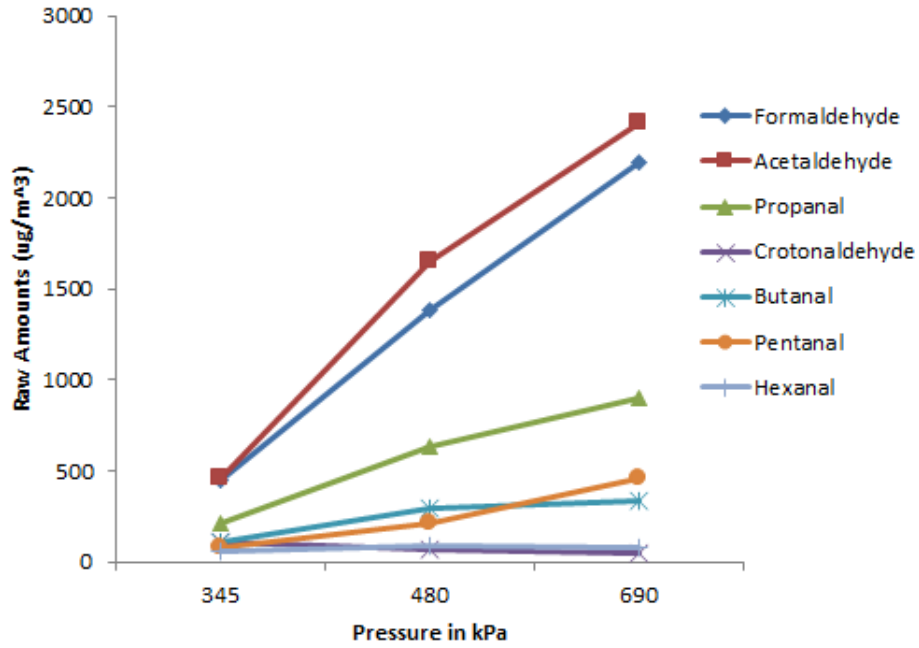
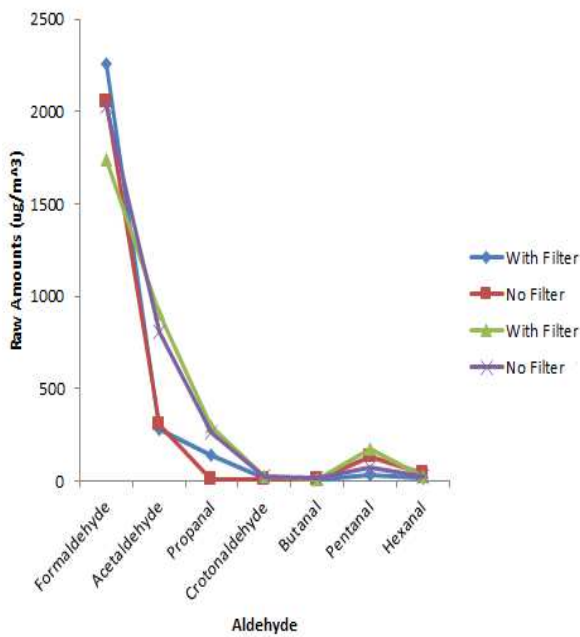


Figure 4.3: Variation of aldehyde concentration for different pressures

Aldehyde Conc. at 280 deg C, 690 kPa



Aldehyde Conc. at 310 deg C, 690 kPa

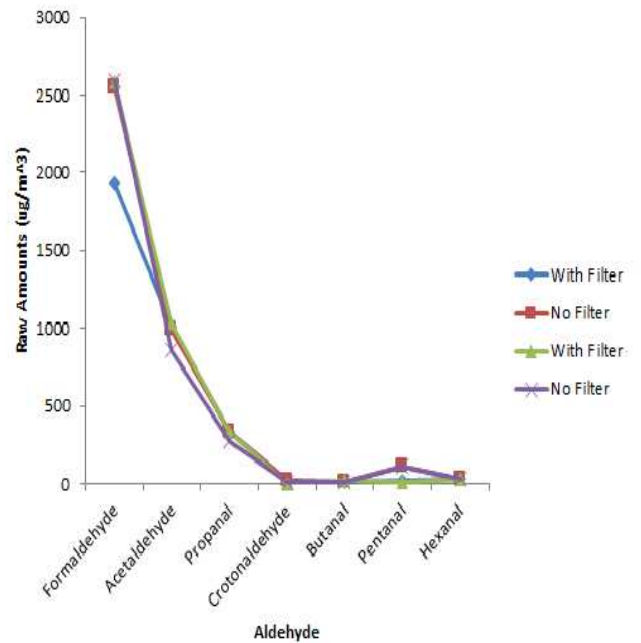


Figure 4.4: Concentration of aldehydes for constant pressure at two different temperatures

Table 4.2: CO concentration for different temperatures and pressures measured by FTIR (units in ppm)

Maximum CO (ppm)		Pressure (kPa)			
		200	345	480	690
Temperature (°C)	185	0	0	0	0
	220	0	0	7	11
	250	8	11	13	16
	280	11	14	15	20
	310	18	20	28	42

The FTIR measurement was made from the bleed air injection line before it was introduced into the simulator duct. It should be noted that, in real aircraft, these values would be reduced by the level of recirculated cabin air. The maximum measured value occurs at the maximum temperature and pressure point and based on typical climb- out time would be less than 90 seconds [19].

Particle size distribution and concentration for the twenty different temperature and pressure conditions are summarized in Figures. 4.5 to 4.8.

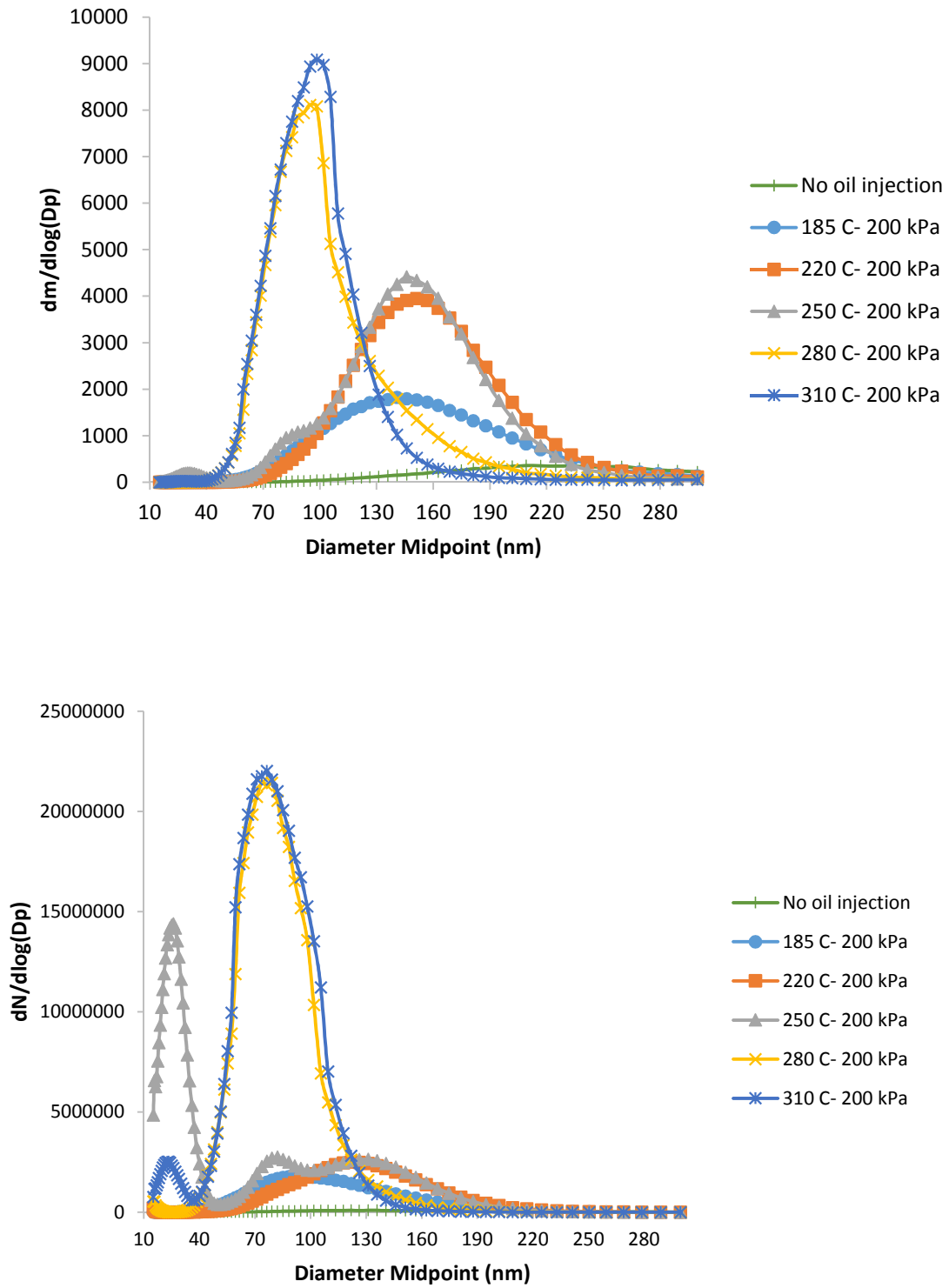


Figure 4.5: Detailed mass and number of concentration data at 200 kPa

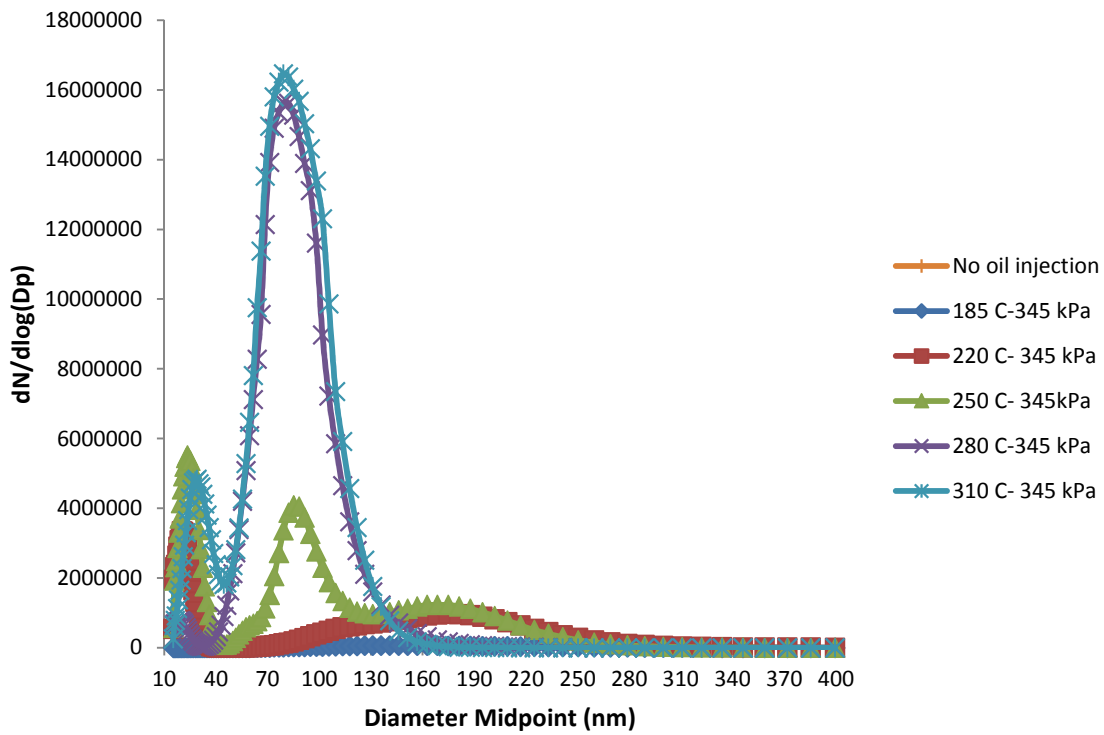
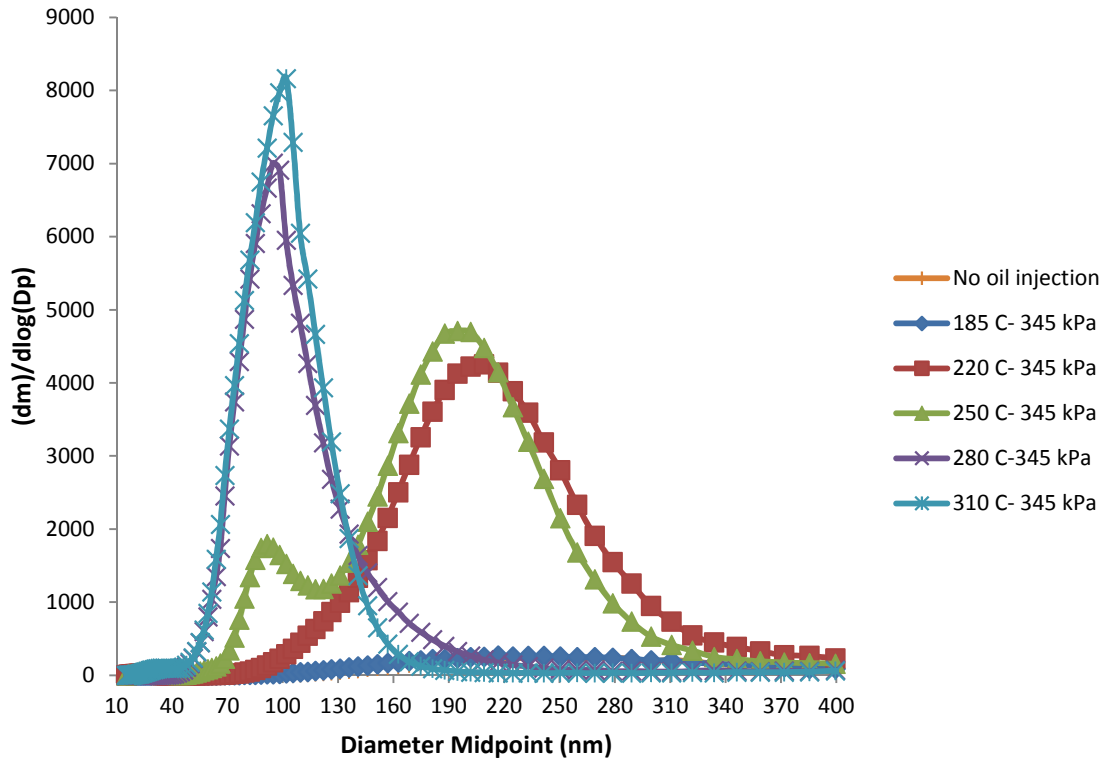


Figure 4.6: Detailed mass and number of concentration data at 345 kPa

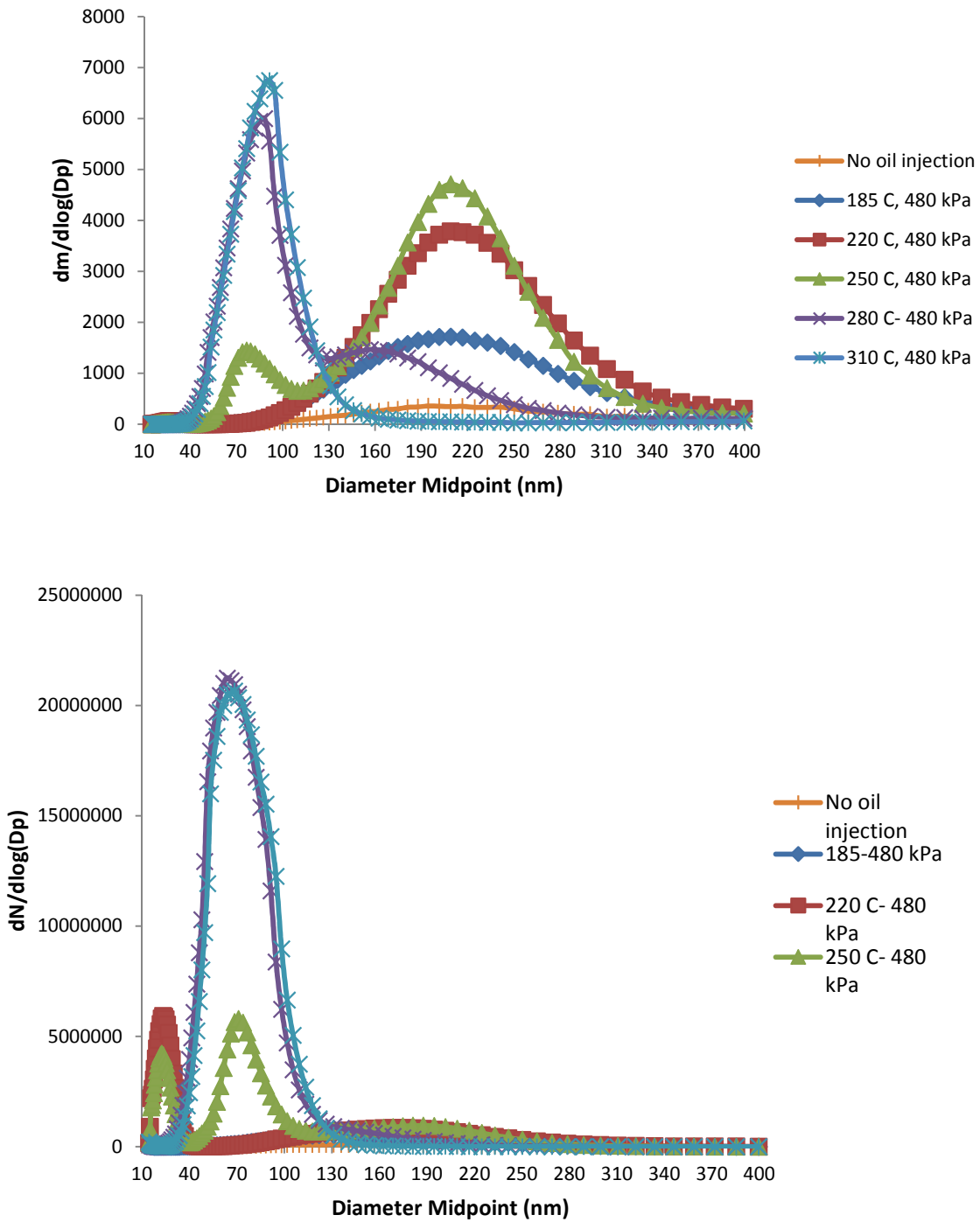


Figure 4.7: Detailed mass and number of concentration data at 480 kPa

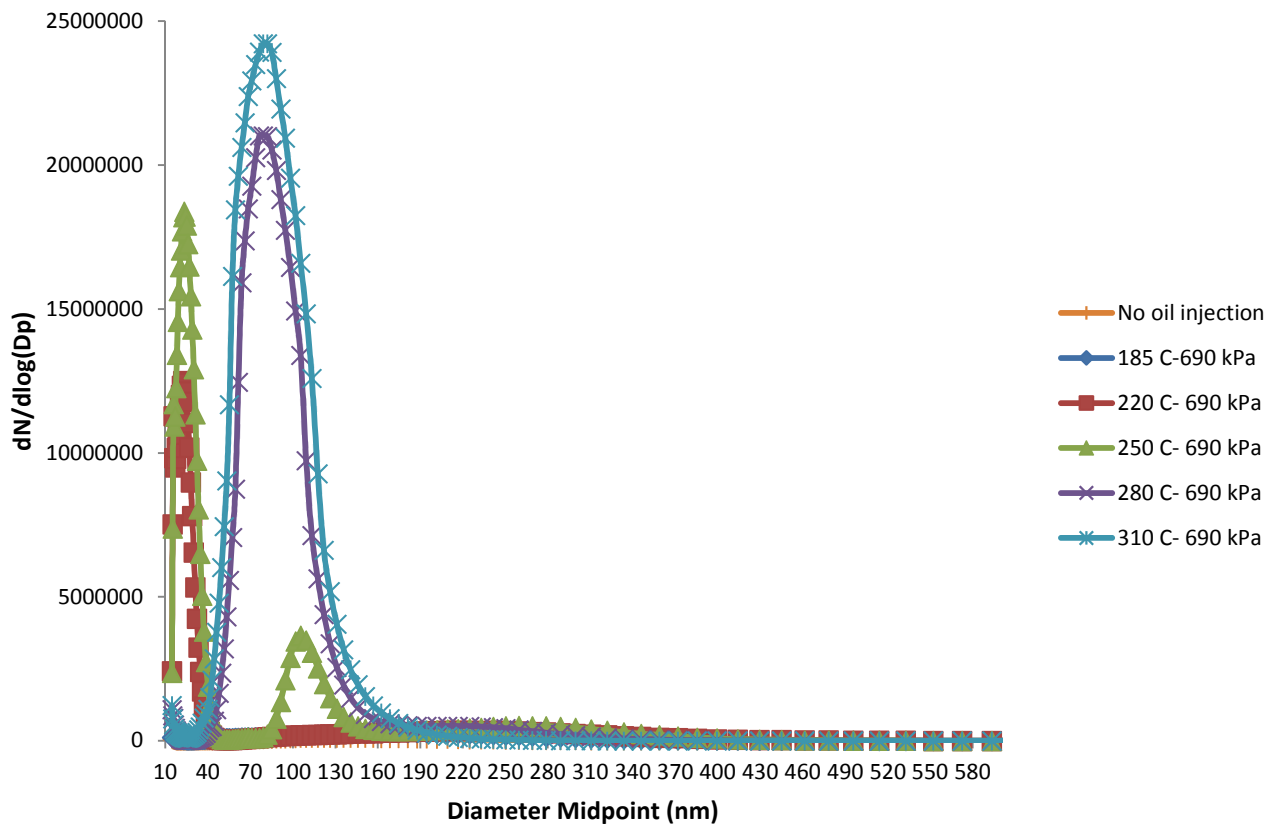
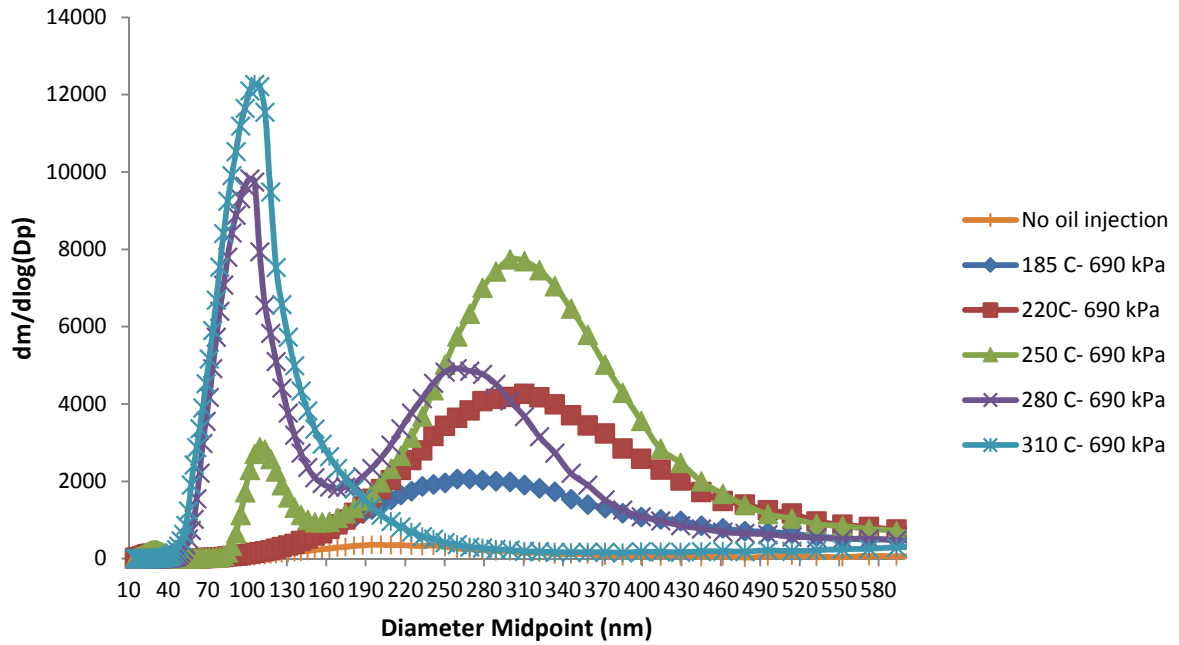


Figure 4.8: Detailed mass and number of concentration data at 690 kPa

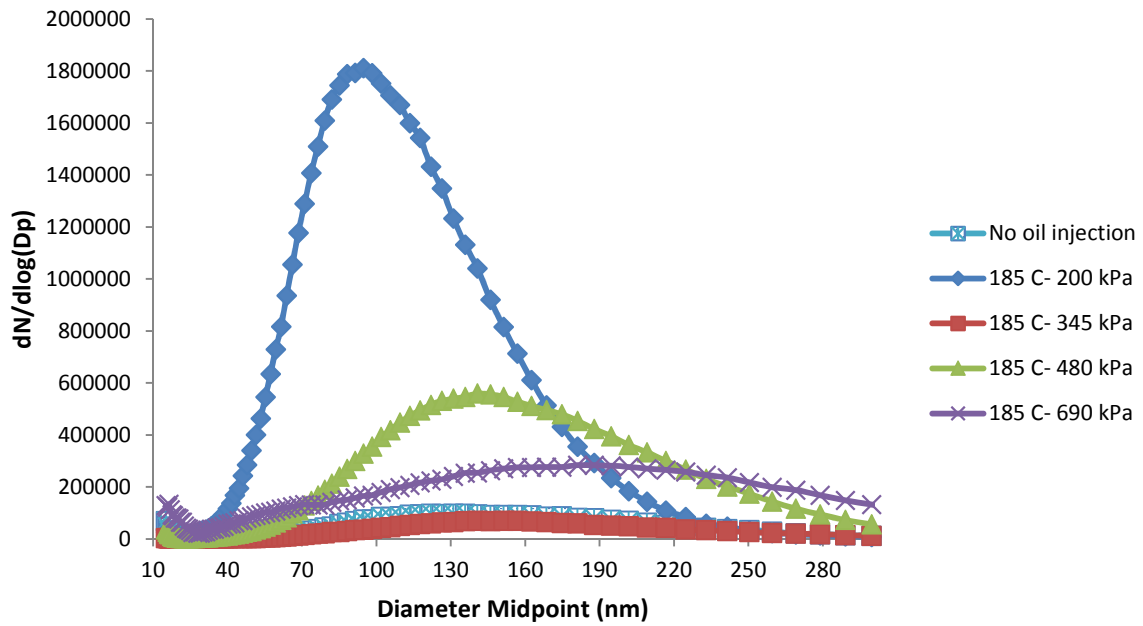


Figure 4.9: Detailed concentration data at 185 ° C

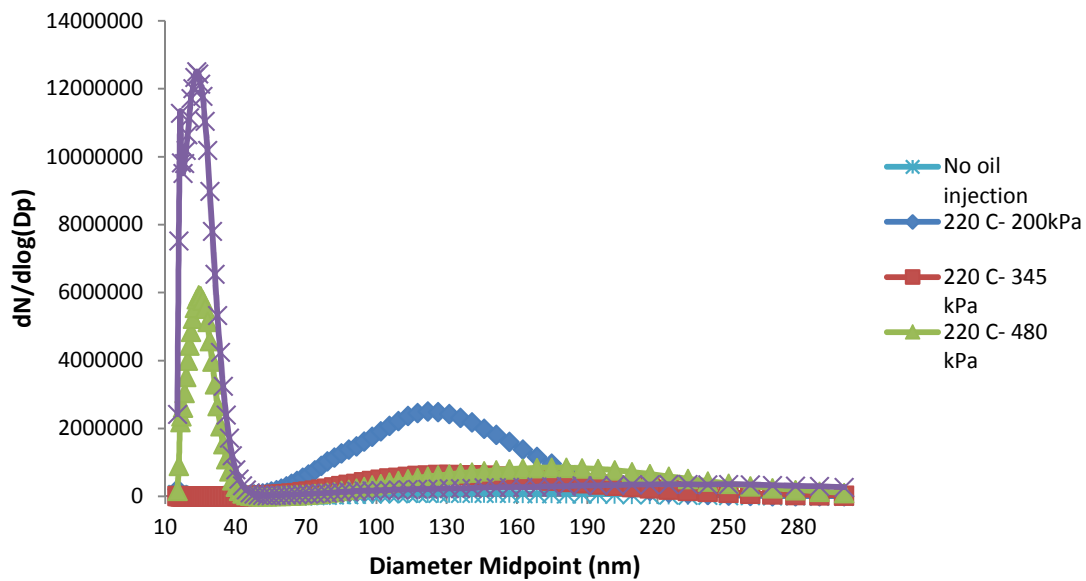


Figure 4.10: Detailed concentration data at 220 ° C

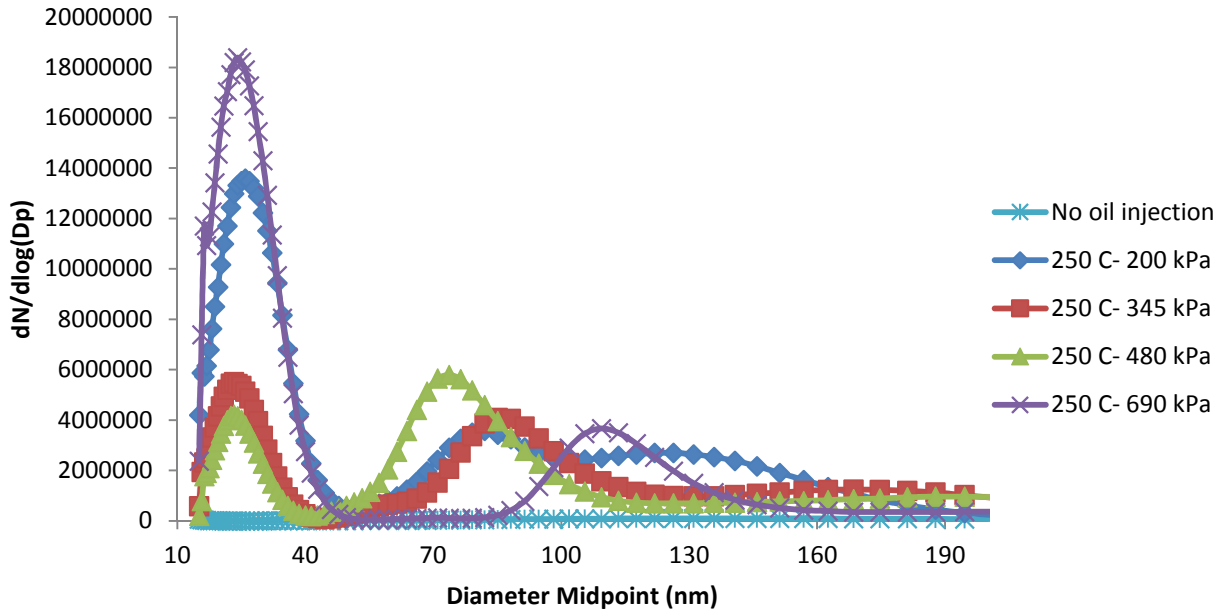


Figure 4.11: Detailed concentration data at 250 ° C

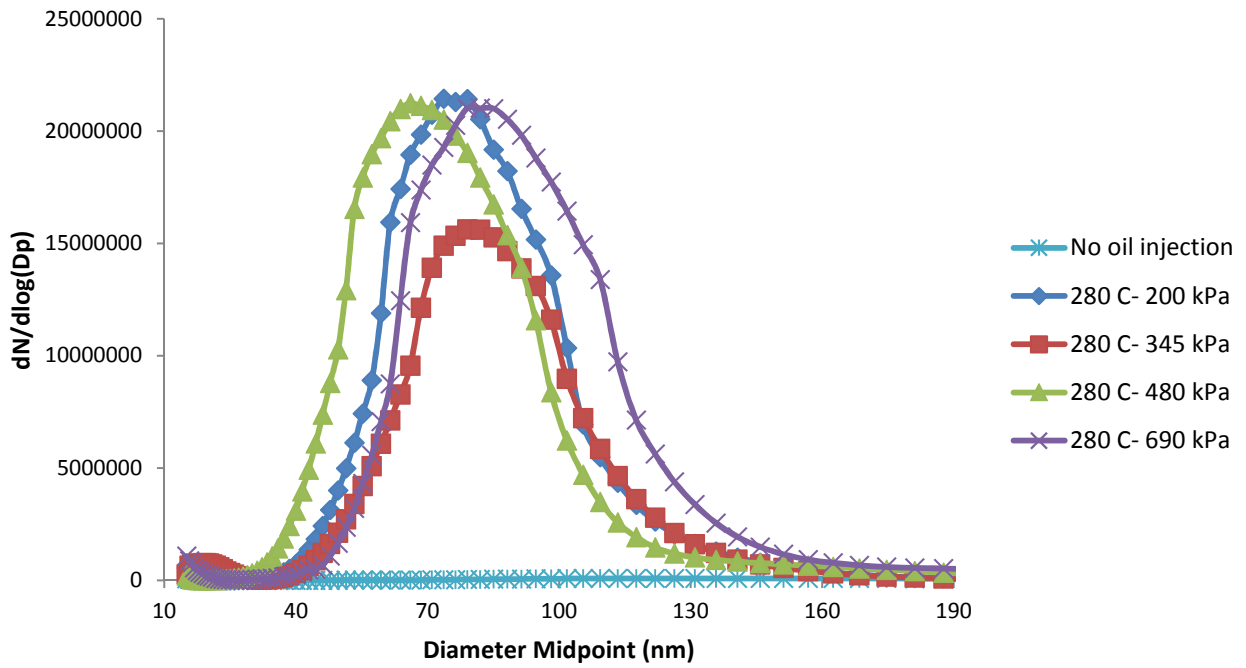


Figure 4.12: Detailed concentration data at 280 ° C

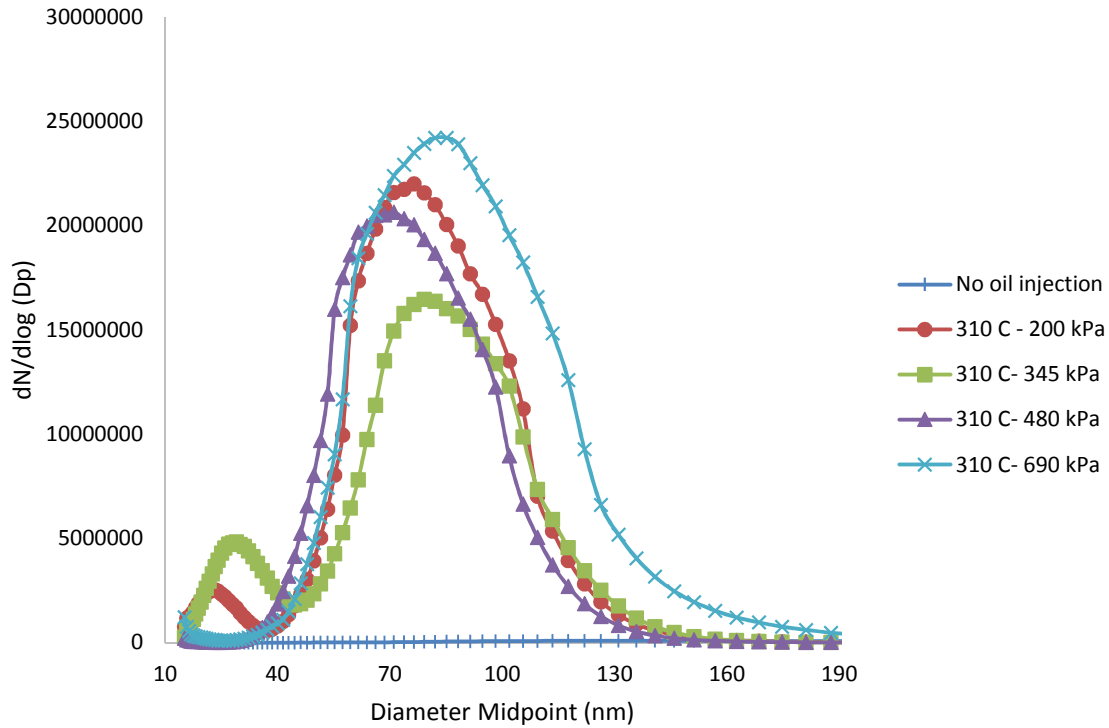


Figure 4.13: Detailed concentration data at 310 °C

As it is seen in from Figures 4.5 through 4.13, particles have their maximum size and minimum number concentration for all pressure at a temperature of 185 °C . Increasing the temperature range to 220 °C to 250 °C , a significant increase in ultra-fine particles takes place and the particles size reach a minimum value. Then, in the temperature range from 280 °C to 310 °C , the reverse behavior is observed and particle size starts to increase and reaches a maximum number concentration at 310 °C . At a temperature range of 186-250 °C , pressure has major effect on the number of particles and size distribution but as temperature increases to a range of 280-310 °C this effect is negligible. Particles have the maximum number concentration at maximum temperature and pressure of 310 °C and 690 kPa, respectively. Concentration versus

time graphs show that, during the time span of each measurement point (constant temperature and pressure), there is no substantial change in the particle size distributions or concentrations.

4.5 Conclusions of This Study

In this research, for various bleed air temperatures and pressures generated by a bleed air simulator, the concentrations of different chemicals as well as the number of particles and size distribution were studied. As a result of the present study the following conclusions may be reached:

1) Aldehydes such as formaldehyde, acetaldehyde, propanaldehyde, crotonaldehyde, butanal, and hexanal are formed and aldehyde production dramatically increased with increasing pressure and temperature in the pressure range of 200- 480 kPa. However at 690 kPa, it only increases with pressure and increasing temperature has minimal effect.

2) CO concentration is increased by increasing both pressure and temperature and reaches a maximum value at the maximum temperature and pressure evaluated, 310 °C and 690 kPa.

3) Results show that, at a bleed air temperature of 185°C, the minimum temperature evaluated, oil particles have a maximum size and minimum number concentration. However, by increasing temperature, there is initially a considerable increase of ultra-fine particles observed then increasing temperature to higher values leads to slightly larger particles and higher concentrations. Finally, the maximum number concentration of particles takes place at the maximum temperature and pressure evaluated (310 and 690 kPa).

4) At temperatures from 185 °C to 250 °C, both bleed air temperature and pressure

have a decisive influence on the oil particle size and concentration but for temperatures over 250 °C the pressure has minor effects.

As a final comment, the question arises as to whether or not a reciprocating compressor followed by a heater provides a realistic representation of bleed air process in an aircraft engine. As will be seen in the following chapter, the characteristics of the particulates in three very different aircraft engines is similar in to those in the bleed air simulator in that ultrafine particles dominate the number concentration of particles. This consistency gives some confidence that the bleed air simulator gives a reasonable representation of aircraft engine bleed air.

CHAPTER 5 - Characterization of Particles Resulting from Oil

Contamination of Aircraft Engine Bleed Air²

Although in Chapter 4 the BAS provided a means to conveniently and carefully provide controlled conditions for assessing oil contamination of bleed air, it has limitations on the reliability with which it simulates bleed air. Especially, it uses a reciprocating shop compressor to compress the air. Since this type of compressor is knowingly cooled to rise the efficiency of compression and avoid the challenges of high temperature operation, the temperature of the air from the compressor is not illustrative of aircraft bleed air at the same pressure. Consequently, a separate heater was required. Aircraft engines use high speed turbo machinery to compress the air and there is no cooling of this air internal to the compressor. The shear mechanisms accountable for aerosol generation may be very different in a reciprocating compressor as compared to an engine compressor. Additionally, the BAS heater raises the temperature through a heat transfer process whereas the temperature increase for aircraft bleed air is due to adiabatic compression. For these reasons, in this chapter, it is preferred to check the results of the BAS with bleed air from a turbine engine.

² Based on: Amiri, S. N., Jones, B., Hosni, Mo., Roth, J. (2018). “Characterization of Particles Resulting from Oil Contamination of Aircraft Bleed Air” Indoor Air Journal, under review

5.1 Experimental Program

This part of the research was conducted in three phases. The experimental facilities for each phase are described in the following sections.

5.1.1 Allison 250 C18 Turbine Engine

For the first stage of this study, an Allison 250 C18 turbine engine was chosen (Figure 5.1). This engine usually powers small helicopters and airplanes and is also used for many land-based applications. It has a nominal power rating of 300 HP (220 kW). The C18 test engine used had an air flow rate at 90% power of approximately 1.36 kg/s and it was able to generate maximum bleed air temperature of approximately 250 °C. The engine compressor has six stages of axial compression and one stage of centrifugal compression. The experimental setup included various components such as the oil aerosol generator, bleed airline, dynamometer; dynamometer coolant loops; oil cooler; and fuel pump. The bleed air system was set up similar to the aircraft installation. Bleed air was extracted for the bleed port on the engine compressor and passed through an aircraft precooler prior to being sampled. An oil aerosol was generated with a bank of TDA-4B lite Laskin nozzles and injected into the engine air inlet at different rates. Sampling ports were available to allow the intake air to be sampled both upstream and downstream of the oil injection. The simplified test setup layout diagram is shown in Figure 5.2 and Figure 5.3 shows the oil injection system. Shop air was used for the aerosol generator and was filtered and dried before being supplied to the generator. A detailed explanation of the test setup has been presented by Roth [18].



Figure 5.1: Allison 250 C18 turbine engine and its test setup

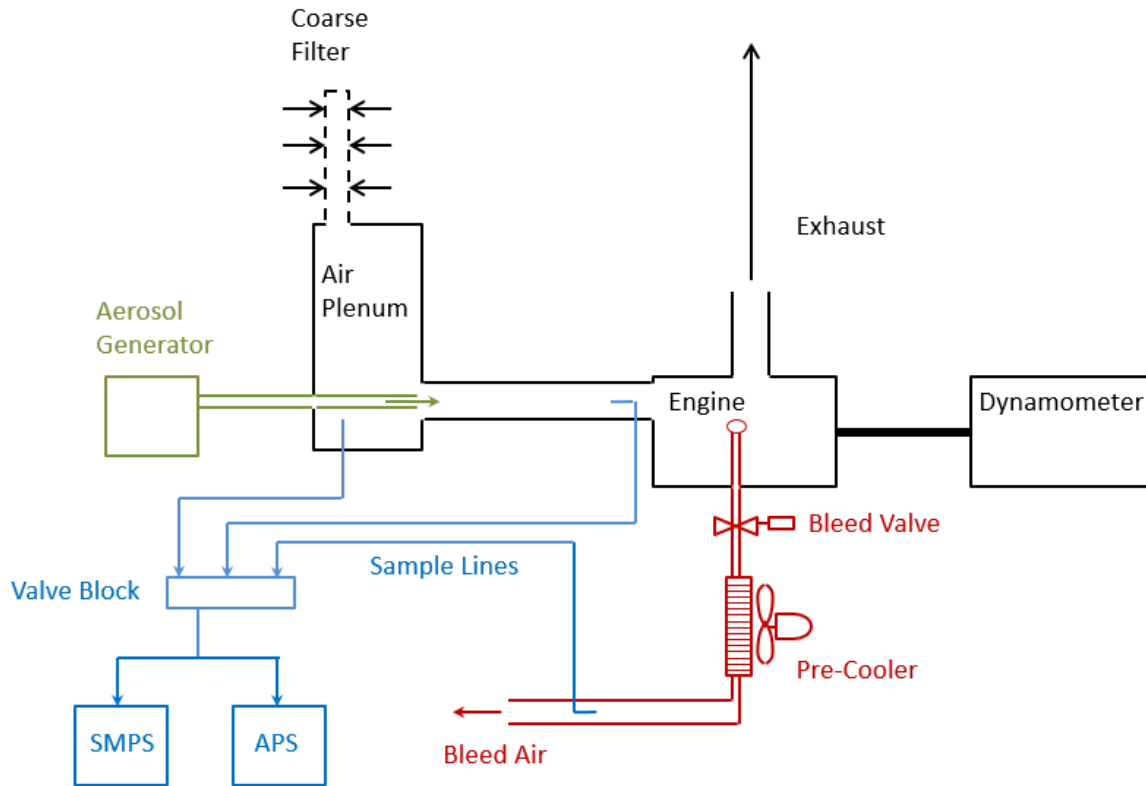


Figure 5.2: Schematic of Allison 250 C18 Turbine Engine, its accessories assembly and test measurement instrument's details



Figure 5.3: TDA-4B lite Laskin nozzle unit, oil injection and sample ports

5.1.2 Allison 250 C28B Turbine Engine

In the second stage of this study, to achieve the temperatures and pressures which are needed to produce thermal decomposition of turbine engine lubricant (Mobile Jet II) and that are representative of typical airliner bleed air conditions, an Allison 250 C28B Turbine Engine (Figure 5.4) was used. This engine had improvements in comparison with the previous generation of Allison 250 engines in compressor, combustor and turbine airflow. The C28 B engine has a nominal power rating of 500 HP (370 kW) and has a single centrifugal stage for compression. By using this engine, bleed air with temperatures up to 320 °C could be generated. Bleed air temperature in typical commercial aircraft, depending on operation mode, can range from 185 °C to 310 °C [19] so this engine covers this range well. The test setup and test measurement instrument's details are same as for the C18 engine shown in Figure 5.2 except that space constraints did not allow the placement of the line that sampled the aerosol laden air of the inlet to the engine.



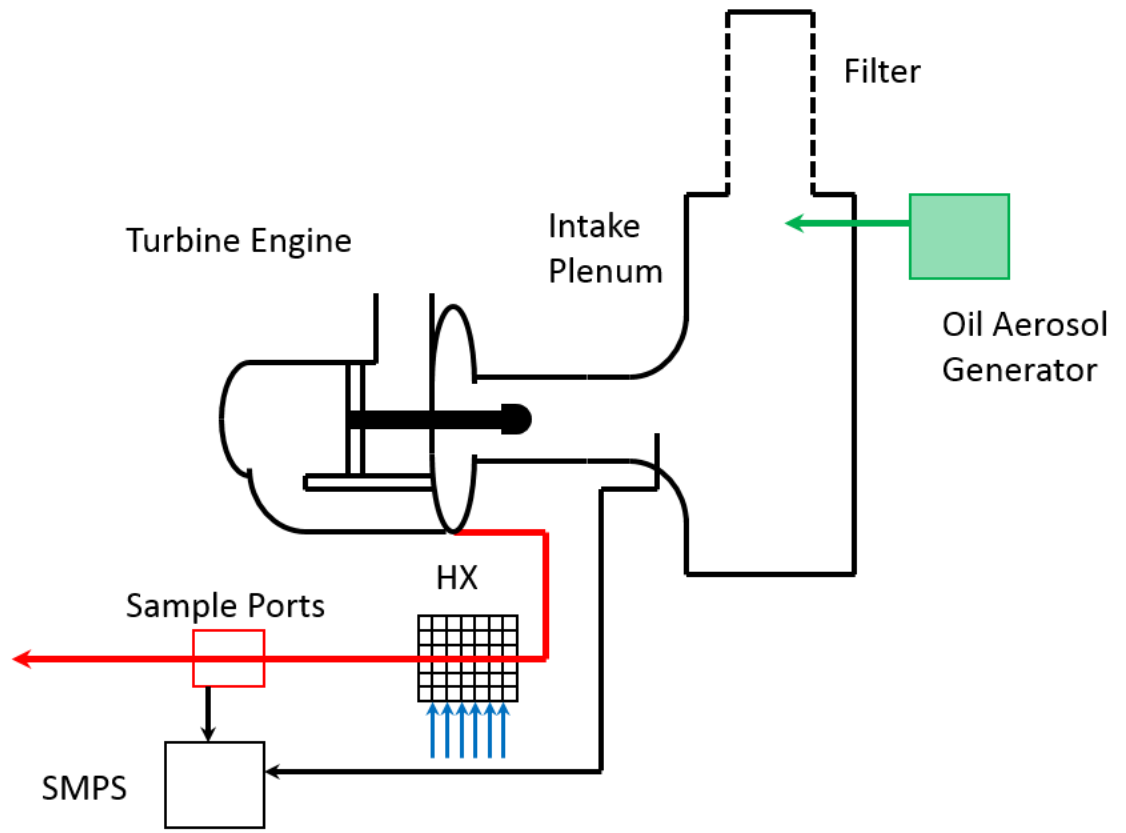


Figure 5.4: 250 C28B Turbine Engine and its field setup

5.1.3 Pratt and Whitney F11/PW2000 Turbine Engine

In the final stage of this study, a series of tests was conducted on a Pratt & Whitney F117-PW-100 engine on-board an Air Force C17 aircraft under nominal and simulated oil contamination conditions. These tests took place at Edwards Air Force Base (EAFB). The particulate measurements were just one part of a much larger experimental program and the test setup was design to accommodate a number of different experiments. The data were collected on the ground from an engine mounted on an operational aircraft. A simplified diagram of the experimental setup

is shown in Figure.5.5. Oil was injected via a nozzle mounted in an inspection port near the front of the compressor. There are two bleed air ports on the engine, the low pressure port and the high pressure port. The engine and bleed air manifold were modified so the bleed airport selected could be controlled remotely. The bleed air was diverted to an instrumentation platform located beneath the engine. The bleed air was cooled in two stages to allow sampling at different temperatures representative of different locations in the bleed air system. The bleed air was cooled using aircraft bleed air pre-cooler heat exchangers. The particulates were sampled at the last stage where the bleed air had been cooled to levels acceptable for the scanning mobility particle sizer spectrometer (SMPS) and aerodynamic particle sizer (APS). The engine was operated at a power level intended to give bleed air conditions representative of cruise operation.

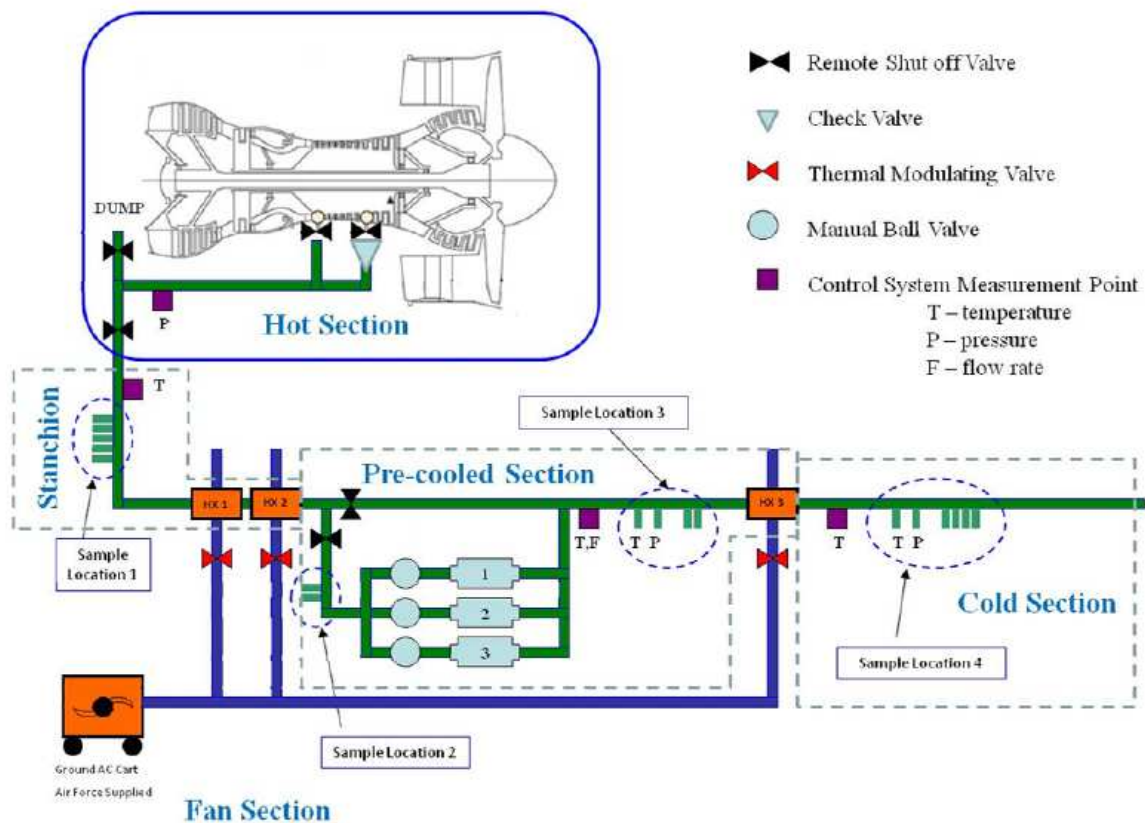


Figure 5.5: Test setup for Pratt and Whitney F11/PW2000 Turbine Engine

In the current study the following devices and measurement systems are used to characterize the bleed air aerosols:

- a) a scanning mobility particle-sizer spectrometer (SMPS) : can measure concentration and size distribution of particles in the range of 10 to 1000 nanometers.
- b) an aerodynamic particle sizer (APS): can measure concentration and size distribution of particles in the range of 500 nanometers to 20 micrometers.

A full description of the instrumentation and measurements employed in this research has been given in the previous study by Nayyeri et al. [13].

5.2. Results and Discussions

The C18 engine test results for the distribution of the number concentration of particles and the distribution of particle mass with respect to particle size are shown in Figures. 5.6 and 5.7. As seen in Figure.5.6, the number of particles increases with temperature (engine speed). Temperatures are nominal values for reference purposes and measured values are typically within 1°C of the nominal value and not more the 2°C from the nominal value. From 115 °C to 145 °C the increase in the number of particles is small. From 145 °C to 155 °C the number of particles increased tremendously, but after 155 °C the increase in the number of particles is again small. It should be noted that the maximum bleed air temperature of the C18 engine is lower than the charring point of the engine oil (Mobil Jet II) temperature. Accordingly, the increasing number of particles with increasing temperature likely is not due to thermal decomposition of oil. Both temperature and pressure in a turbine engine compressor increase together with engine speed and engine power. As is seen in Figure. 5.7 at lower temperatures (engine speeds) (from 115 °C to 165 °C), the mass is located in bigger particles and then, as the temperature (engine speed)

increases, the larger particles apparently are sheared into smaller particles. Considering that there is a cubic relationship between mass and diameter, the same amount of mass may result in a couple of orders of magnitude increase in particle numbers when they are sheared into smaller particles. According to the C18 engine data, the bulk of particles by number is less than 150 nanometers in diameter except perhaps at the lowest power levels. The power levels would correspond to engine idle operation.

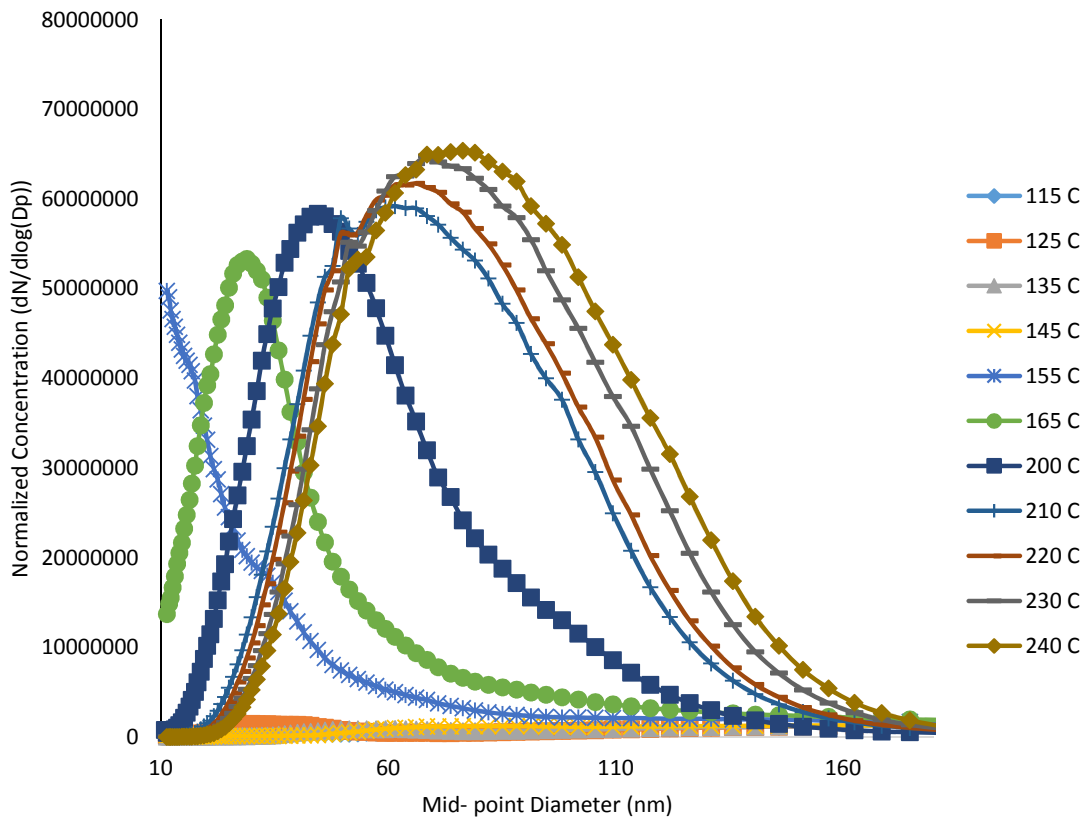


Figure 5.6: Distribution number of particles respect to particle diameter for C18 engine

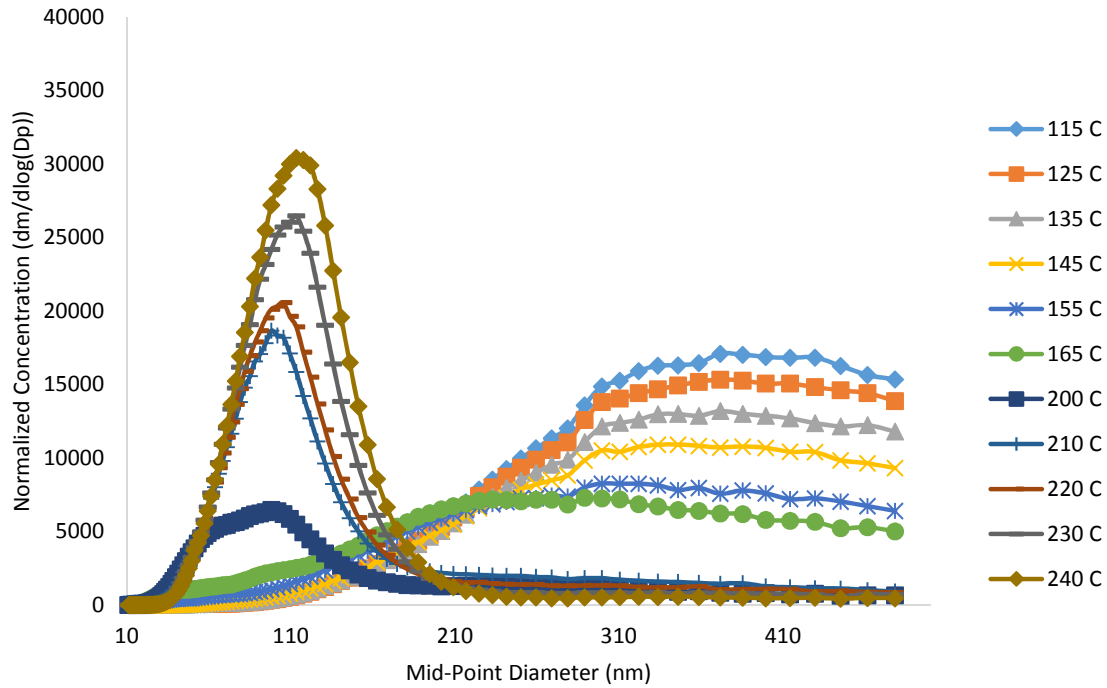


Figure 5.7: Distribution of particles mass respect to particle diameter for C18 engine.

Because the temperature conditions that could be achieved with C18 engine were less than those that would be expected in typical commercial aircraft bleed air system and are also less than the charring point of oil, in the second stage of this research, the C28B engine was used and data collected on the same test stand. This engine is capable of generating bleed air pressures and corresponding temperatures in the range typical of large aircraft engines. As it is seen in Figure. 5.6 and Figure.5.8, there is reasonable agreement between the results obtained from C18 and C28B engines at 240°C with the C28B engine generating slightly smaller particles. The C28B data in Fig.5.8 show that additional increases in temperature (engine speed) have only a small effect on the size particles generated. Figure.5.9 indicates similar conclusions can be drawn about the mass distribution at the higher temperatures.

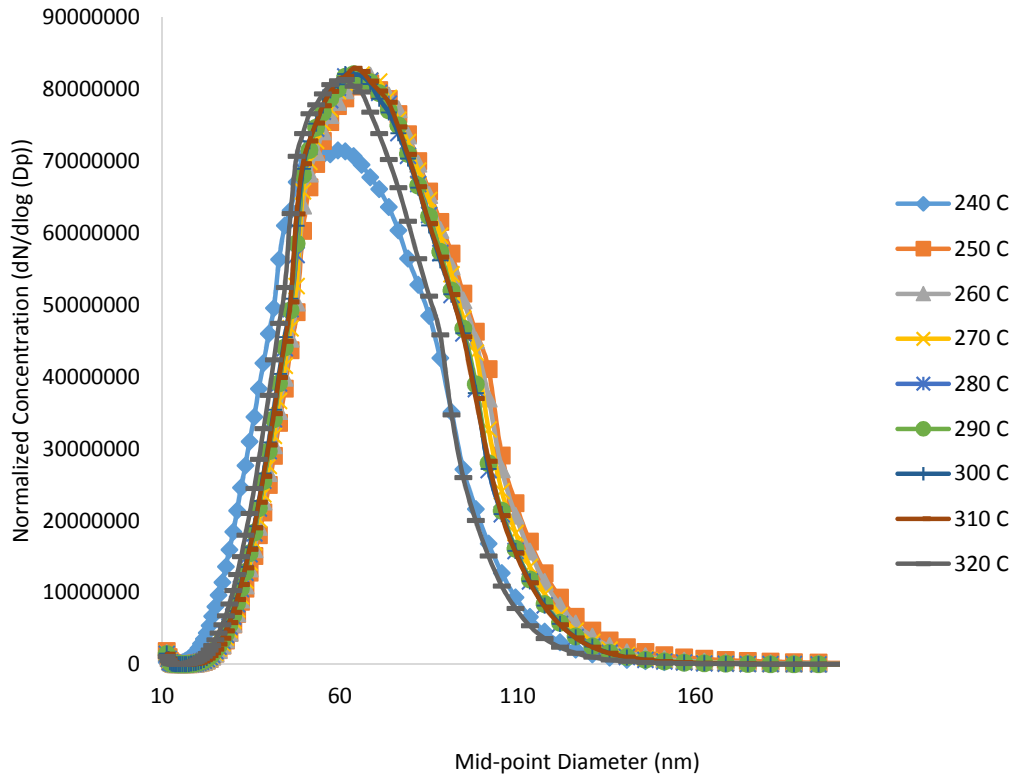


Figure 5.8: Distribution number of particles respect to particle diameter of C28B engine

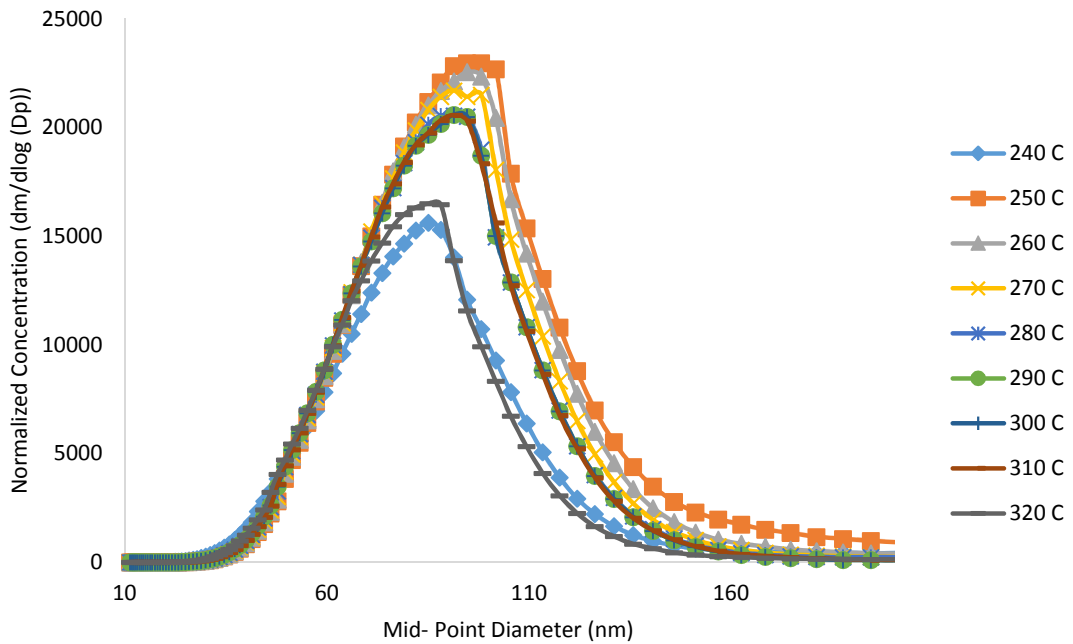


Figure 5.9: Distribution of particles mass respect to particle diameter for C28B engine.

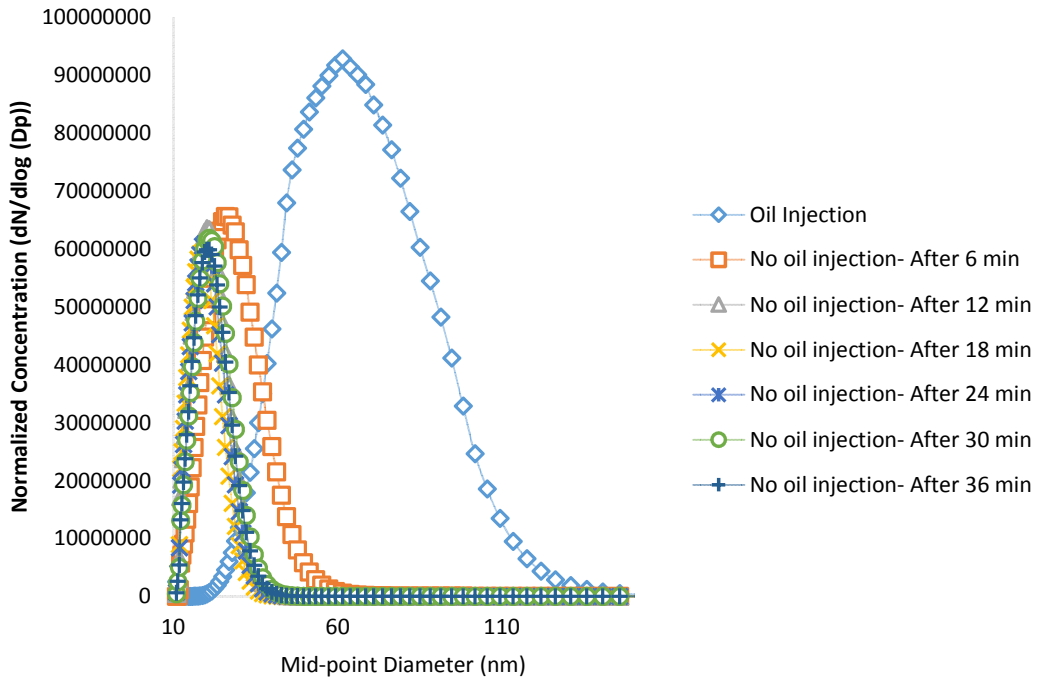


Figure 5.10: The decay trend of number of particles for C18 engine

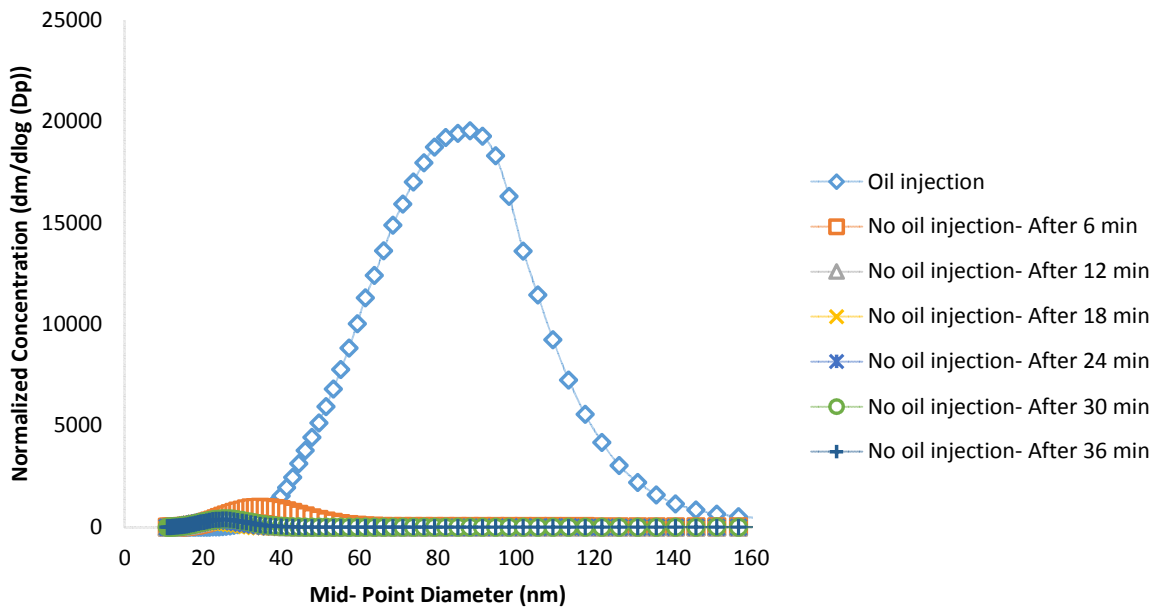


Figure 5.11: The decay trend of particles mass for C18 engine with different numbers of nozzles

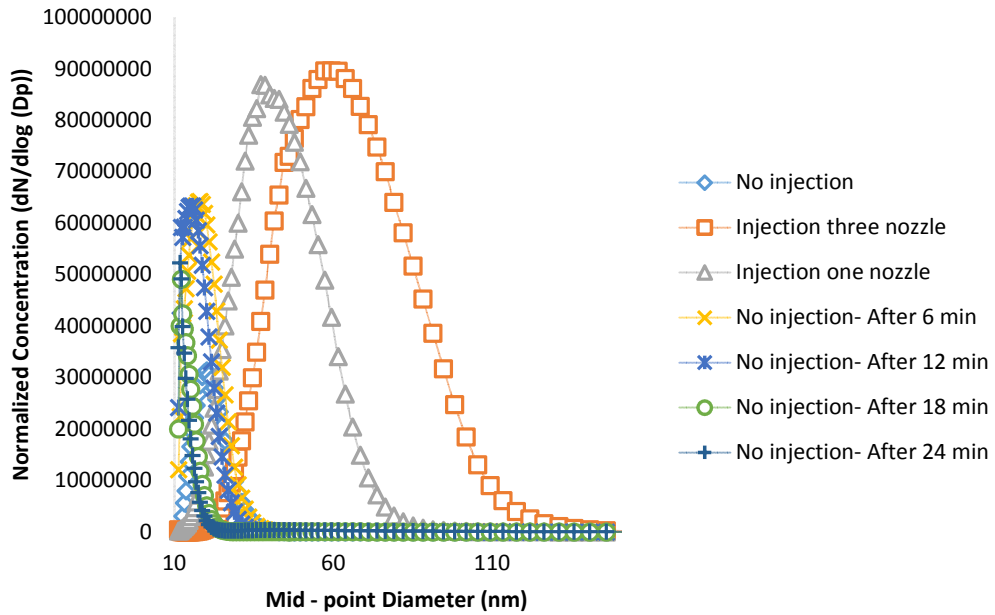


Figure 5.12: The decay trend of number of particles for C28B engine with different numbers of nozzles

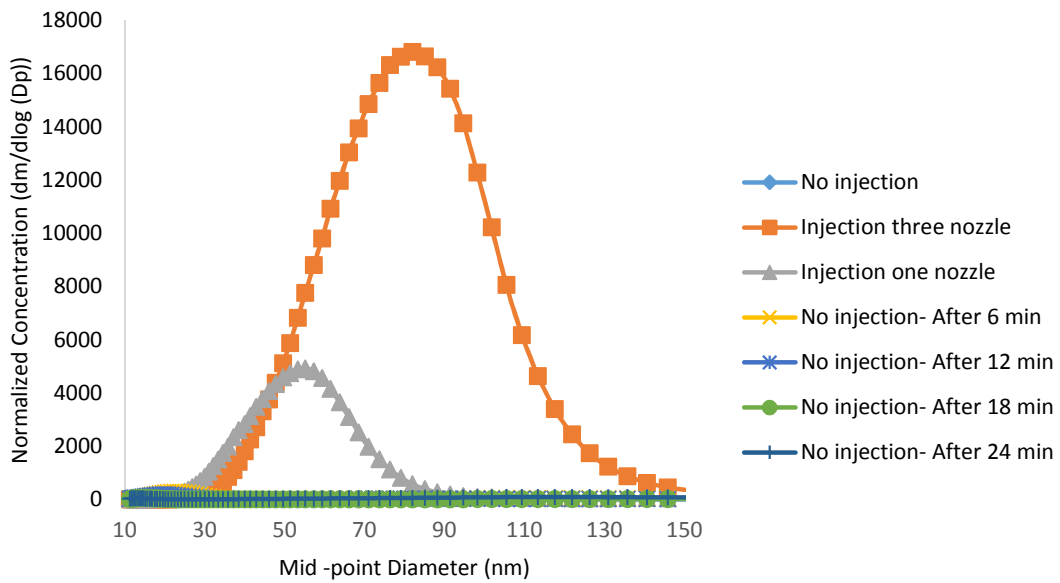


Figure 5.13: The decay trend of particles mass for C28B engine with different numbers of nozzles

To insure that valid steady state data were being collected, tests were conducted to determine how long of a time period was required for the particle size distribution to reach a steady state when the injection rate was changed. When injection was started on a running engine, steady state was achieved almost instantly, within the time resolution of the SMPS. The SMPS requires about 135 seconds to complete a scan and generate a size distribution. After the first scan, little change was seen in the size distribution. However, upon turning off the injection, a much different phenomenon was observed. Figure. 5.10 and 5.11 show the decay behavior for the C18 engine and Figure. 5.12 and 5.13 show the decay behavior for the C28B engine. In both cases, the presence of particles does not stop immediately after cessation of oil injection. Rather, the size gets smaller and smaller while the number concentration decreases modestly, at least initially. With the C18 engine, the distribution eventually stabilizes with a peak concentration around 20 nanometers and does not continue to decrease. This result indicates the possibility of a very small oil leak in that engine or it could have been from the ingestion of exhaust on that particular day. However, the stability of the distribution argues for the former explanation as exhaust ingestion is subject to wind currents and tends to be erratic. With the C28B engine, the initial behavior is similar but the size keeps getting smaller and smaller until it more-or-less passes below the detection range. Figures. 5.11 and 5.13 show that the mass present drops off very quickly because of the decrease in size of the particles.

The decay tests indicate that there are residual oil films in the compressor that are dissipated slowly as aerosol particles are shed with the particles getting smaller and smaller as the films become thinner. Additionally, tests were conducted to determine whether or not the rate of oil injection affected the particle size as well. The oil aerosol generator consists of a bank of three identical venture aerosolizing nozzles and could be operated with one, two, or three nozzles

generating aerosols. Unless mentioned otherwise, all data for this research were collected with all three nozzles operating. The effect of the rate of oil injection on particle size was explored by comparing operation with all three nozzles and with just one. The data for these tests are included in Figures 5.12 and 5.13. By decreasing the injection rate by a factor of three, the peak number concentration decreases from about 60 nanometers to about 40 nanometers with only a modest decrease in the number concentration. The cube of 40/60 is roughly equal to 0.3 and therefore a decrease in size from 60 to 40 nanometers results in approximately the same number of particles even though the amount of contamination is only one third as great.

In the last part of this research, a series of experiments were performed at Edwards Air Force base in the Mohave high dessert. Data were collected from a Pratt & Whitney F117-PW-100 engine on an Air force C17 aircraft as part of the NASA Vehicle Integrated Propulsion Research (VIPR) program. A custom bleed air manifold was installed on the aircraft to allow bleed air to be extracted and piped to an instrumentation platform beneath the engine. The extracted bleed air was cooled by precooler heat exchangers identical to those used on the aircraft but mounted beneath the platform. The cooled bleed air was then sample to determine particulate concentration distributions using the same SMPS as used in the previously described research. Heated oil was injected via a custom atomizing nozzle mounted in the inspection port on the first stage of the compressor (AP1 port). All measurements were conducted on the ground with the engine operating so as to produce bleed air conditions representative of cruise flight. The same engine model is used on the B 757 aircraft. Thus, these experiments are representative of commercial passenger aircraft as well as military transport aircraft.

The results from the third part of the study were measurements were conducted on the C-17 aircraft engine are shown in Figures 5.14 through 5.17. In each figure, two plots are shown. One shows the full range of results and the other uses a highly expanded vertical scale to allow examination of the data with no oil injection. Also, note that the size scale for mass distribution has a larger range than for the number distribution. Even with the lowest injection rate, the number of particles present increased by three to four orders of magnitude as compared to the no oil injection rate. Somewhat surprising, the number of particles present in the bleed air with no oil injection was noticeably lower than the number of particles present in the ambient air. It appears that many of the particulates in the ambient air are removed in the compressor or at least do not get into the bleed air. This result should not be too surprising as fouling of compressor blades is a common concern for turbine engines and ground based engines typically operate with air filters to minimize this problem.

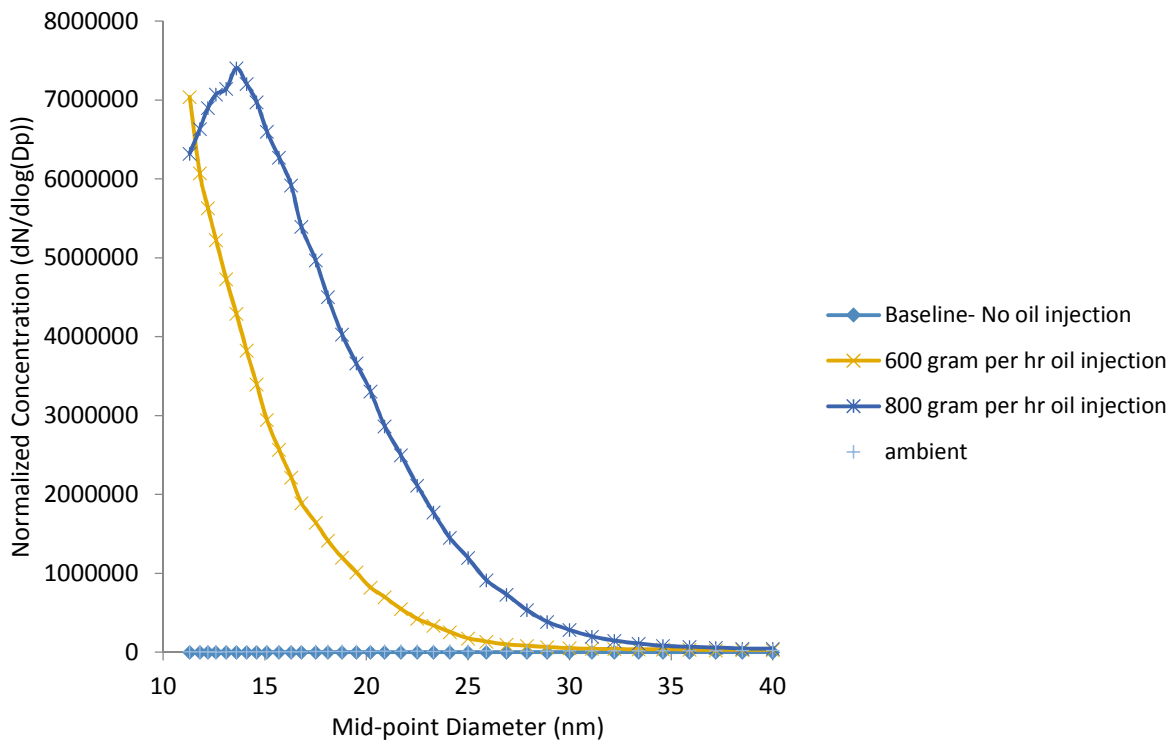
It is seen that the particle size decreases markedly with decreasing injection rates. The peak concentration occurs at approximately 60 nanometers at 1200 grams/hr and decreases to 10 nanometers or less at 600 grams/hr. Also, the total number of particles present increases markedly with the highest injection rate. Multiple measurements of the ambient concentrations were made while the 1200 gram/hr data were collected. Some variability was seen in the ambient values which would be expected. The aircraft was oriented to be pointed into the prevailing wind for these experiments. The one particularly high ambient concentration was likely due to shifting winds which may have resulted in re-entrainment of some engine exhaust.

From the viewpoint of particle size distribution and the number concentration with oil contamination, good agreement is observed between the Air Force C17 data and those collected

from C28B engine. The number concentrations peak at about 65 nm and 55 nm for the C28B and C17 engines, respectively. Similarly, the mass concentrations peak at about 85 and 75 nm respectively. In both cases, the bulk of the particles are in the 20-120 nm range. This consistency gives some confidence that the results are general and give sound guidance as to the nature of particles that would be expected with these levels of contamination. Because the C28B and C18 engine experiments were conducted in an industrial park and the configuration was such that re-entrainment of the engine exhaust could not be completely prevented, the no-oil total particle concentrations in the bleed air for those engines were higher than Air Force C17 engine. Also, the Air Force C17 engine had been thoroughly reconditioned specifically for the purpose of this research program while the C28B engine and, particularly, the C18 engine were well worn, high time engines and possibly had some internal oil leakage.

Contrary to the results of Mann [10] and Amiri [19] where data were collected using a bleed air simulator, no evidence of particle generation by smoking from the oil was seen in the current study. The particle distributions from the bleed air simulator was bimodal at the highest temperatures indicating a separate particle generation mechanism, possibly smoke. Particle distributions measured in the current study were all smooth and single modal at the higher temperatures. There are at least two explanations for this difference. In the bleed air simulator used in the Mann and Amiri studies, the oil laden air was heated to its final temperature in an in-line tube heater after it was compressed. In this arrangement, the tube wall surfaces are necessarily at a temperature higher than bulk temperature of the air. Whereas the reverse will be true in an engine compressor where the elevated temperature is generated entirely by compression and, if anything, there is cooling at the walls. It is possible that the apparent smoke particles were generated at the hotter wall surfaces in the bleed air simulator. It is also possible that smoke is, in fact, generated at the higher

temperature in the engines as well. It is believed that particles in the air impact surfaces within the compressors and are re-sheared from the resulting oil films on the surfaces. The smoke particles are expected to behave similarly and would be suspended in the oil films and, consequently, embedded in droplets sheared from the surfaces. Consequently, they would not appear as separate particles.



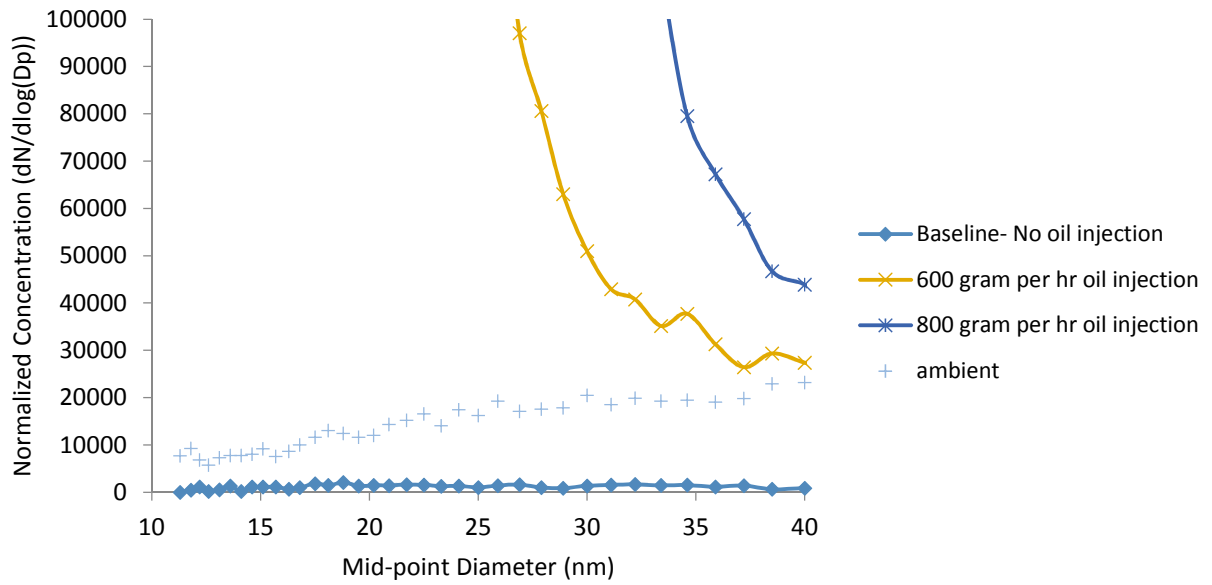
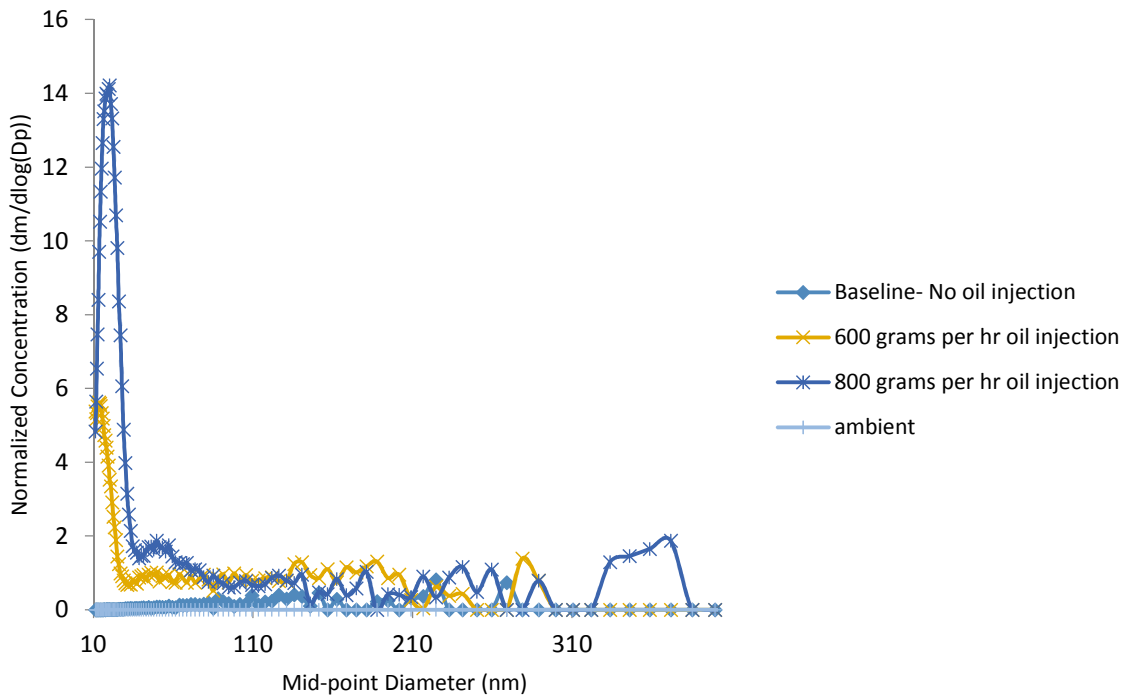


Figure 5.14: : Distribution number of particles respect to particle diameter for Air Force C17

Aircraft



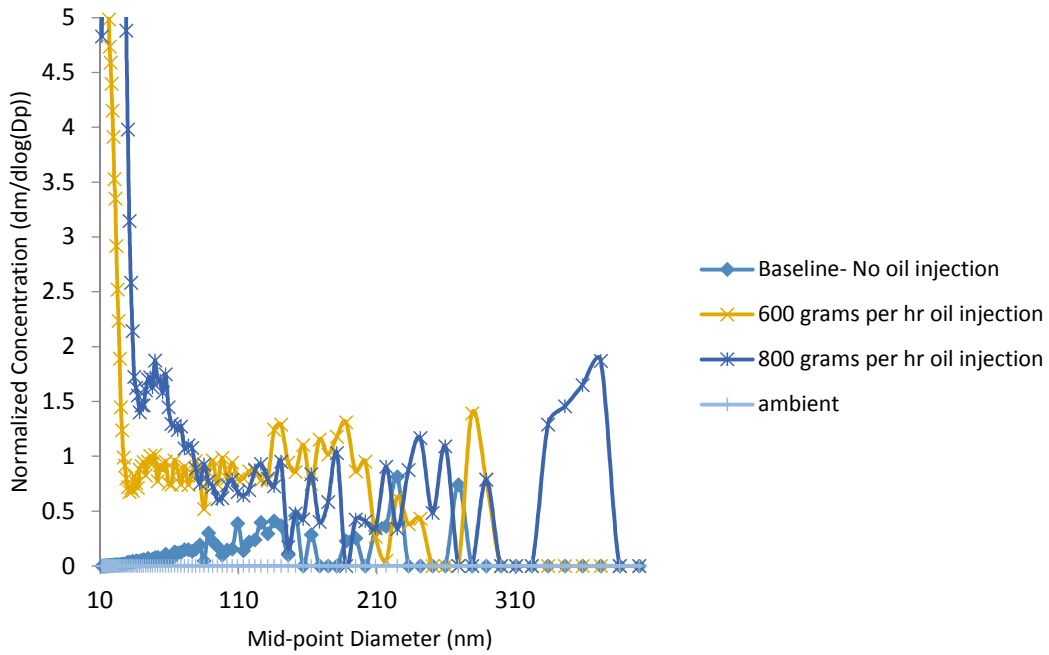
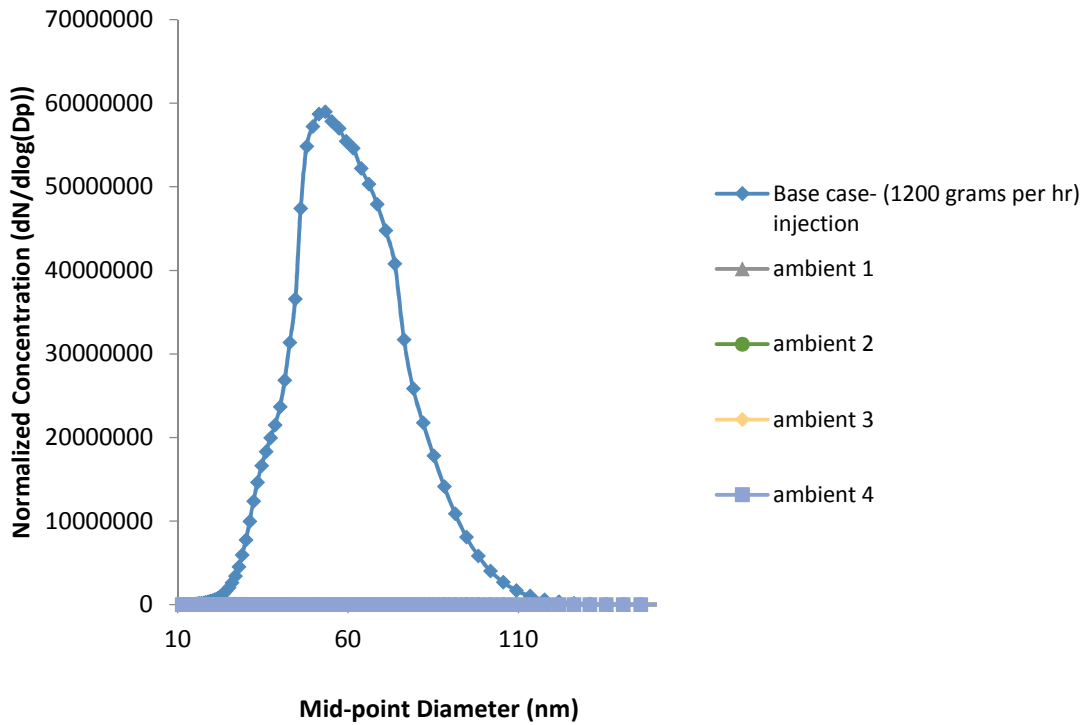


Figure 5.15: : Distribution of particles mass respect to particle diameter for Air Force C17 Aircraft



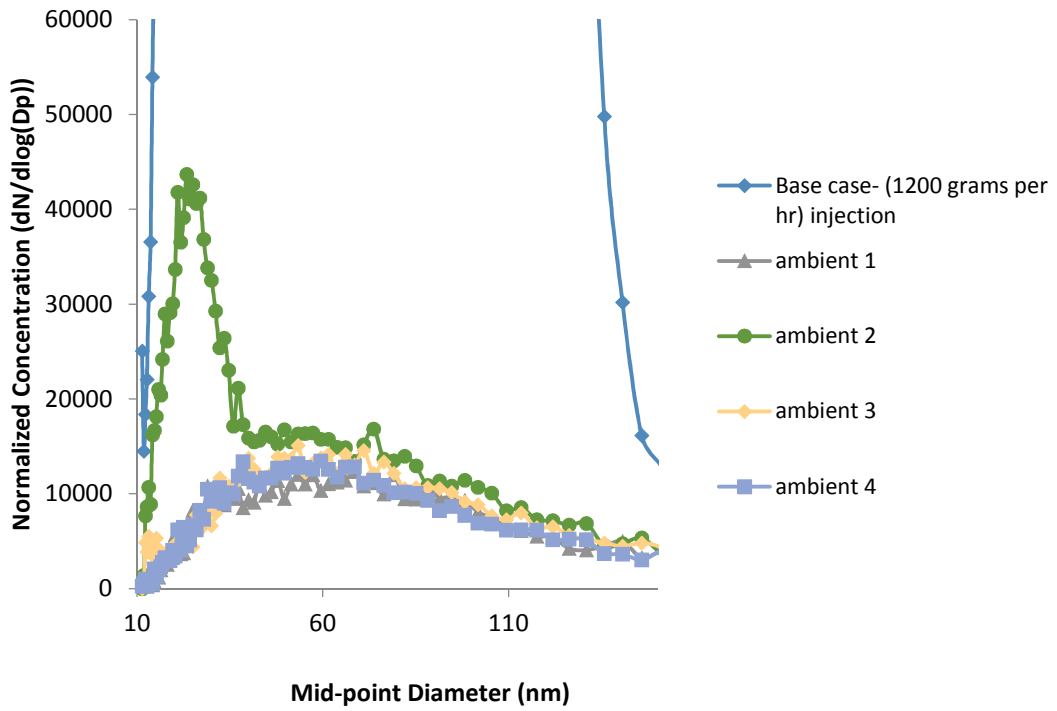
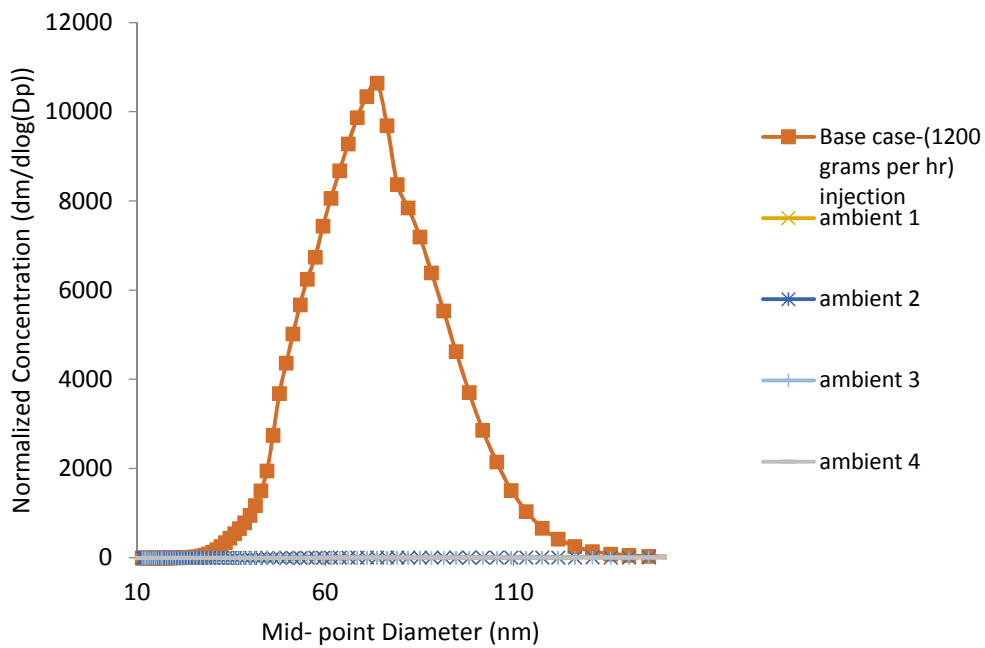


Figure 5.16: : Distribution number of particles respect to particle diameter for Air Force C17 Aircraft



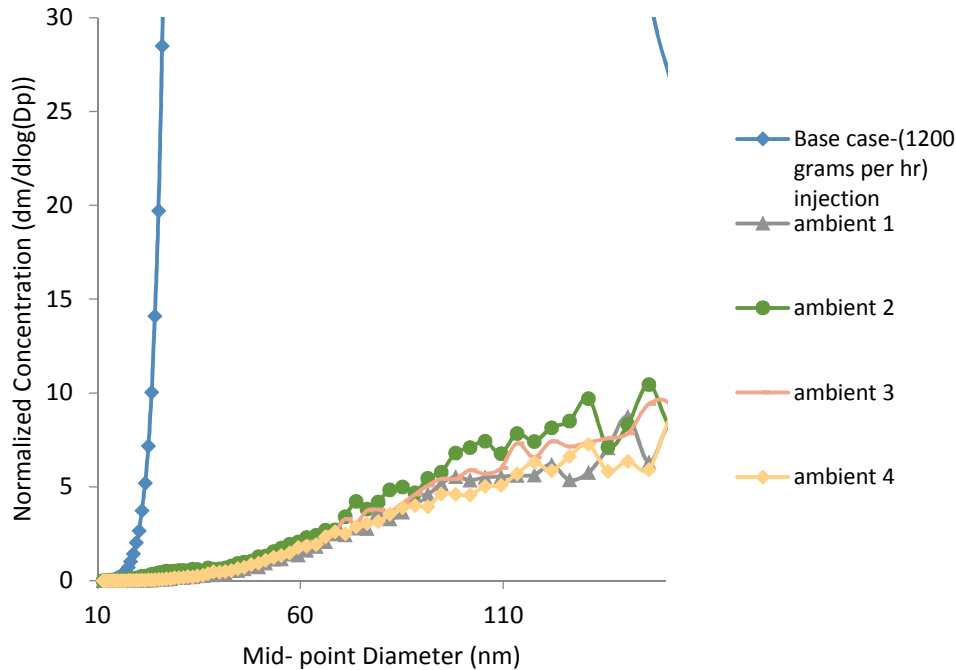


Figure 5.17: : Distribution of particles mass respect to particle diameter for Air Force C17 Aircraft

5.3. Conclusions from This Study

Data collected from all engines (i.e. C18, C28B and Pratt & Whitney F117-PW-100 engines) have good agreement and various independent experimental apparatuses provide mostly consistent result. This consistency shows that the data are representative of aircraft turbine engines and do not depend on a specific make and model of engine. Test results show that at very low power levels (lower engine speeds) particles appear to pass through the compressor more or less untouched and at higher power levels (higher engine speeds), the particles appear to be removed by the compressor and oil films generated from deposition are re-sheared to generate new particles. Normally, oil contamination tremendously increases the number of particles in the bleed air and they are nano-sized particles which have peak concentrations in the range of 50 to 70 nanometers and the bulk of the particles are less than 150 nanometers. In addition, these data indicate that

there should be no difficulty in detecting substantial oil contamination events through particle detection during these events. On the other hand, detection of a low level of leakage before it creates a severe fume event and becomes a critical flight situation, is desired. The data collected in this research indicate that readily measureable particle numbers are likely to be present with low-level contamination but the particle sizes may be exceedingly small, perhaps in the range of 10-20 nanometers and even smaller.

CHAPTER 6 - Conclusion and Recommendation for Further Research

Possible oil contamination of aircraft bleed air is an ongoing operational issue for commercial aircraft. A sensitive and reliable method to detect contamination, especially at very low levels, has been elusive due, in part, to the lack of information about the physical nature of oil that results when entrained in the bleed air by an engine compressor. While it was expected that high shear rates in the compressors would result in very finely dispersed particles, detail data on the size characteristics of these droplets were not available making it difficult to develop reliable detection techniques. The goal of the reported research was to collect experimental data to provide this information. The concentration and size distribution of particles were measured for bleed air with different rates of controlled oil contamination under various engine operating conditions.

Multiple contamination levels were generated by injecting jet engine lubricating oil into the air intake of two different turbine engines (Allison 250 C18 and Allison 250 C28B). The resulting contaminated bleed air was cooled and sampled. In addition, another series of tests was conducted on a Pratt & Whitney F117-PW-100 engine on-board an Air Force C17 aircraft with oil injected into the first stage of the compressor.

Data collected from all engines (i.e. C18, C28B and Pratt & Whitney F117-PW-100 engines) have good agreement in that the particles that are present in bleed air. As a result oil contamination are very small, typically less than 120 nm with peak number concentrations in the range of 50-70 nm with the higher power levels. Given the objectives of this study, these results give guidance as to the size and concentrations that should be expected when detecting these levels of oil contamination. Given the disparity in the size and design of the engines, this consistency

gives confidence that the results are general and not unique to one specific make and model of engine.

Test results show that at very low power levels (lower engine speeds) particles appear to pass through the compressor more or less untouched and at higher power levels (higher engine speeds), the particles appear to be removed by the compressor and oil films generated from deposition are re-sheared to generate new particles. These data indicate that there should be no difficulty in detecting substantial oil contamination events through particle detection in the bleed air. On the other hand, detection of a low level of leakage before it creates a severe fume event and becomes a critical flight situation, is desired.

The data collected in this research indicate that readily measurable particle numbers are likely to be present with low-level contamination but the particle sizes may be exceedingly small, perhaps in the range of 10-20 nanometers and even smaller. However, the low-level oil contamination was not thoroughly examined in this study and it is recommended that additional experiments be conducted to more thoroughly establish lower limits for oil contaminant detection. In particular, the size and concentration as a function of contamination rate should be established and likely background levels with no contamination during flight operations should be established as these background levels may well determine the lower detection limit.

This study used sophisticated laboratory equipment to characterize the particulates resulting from controlled oil contamination of bleed air. The instrumentation is expensive, requires regular servicing, uses a flammable chemical (butanol), has constraints on operating conditions (e.g. the CPC cannot be tipped or jostled), and requires a skilled technician to operate the equipment and interpret the data. It is not suitable for routine use on operating aircraft. For the detection purposes, less sophisticated should suffice. It is recommended that research and

development be conducted to identify and adapt available technology that is suitable for routine use and permanent installation on commercial aircraft.

The contribution of this research to the aircraft engine environment field of research is as follows. Prior to the research reported here, there were no published data available to indicate whether or not particle measurement is a good candidate for detecting oil contamination in the bleed air. The results show that even low oil contamination in the bleed air will produce a large number of ultra-fine particles. Given a large number of particles generated with oil contamination in bleed air, it is now clear that particle measurement, ultrafine particle measurement in particular, is, in fact, a good means of detecting oil contamination in the bleed air.

References

- [1] Magoha, P. (2012). Incident-response monitoring technologies for aircraft cabin air quality.
- [2] Michaelis, S. (2011). Contaminated aircraft cabin air. *J. Biol. Phys. Chem*, 11, 132-145.
- [3] Shehadi, M., Jones, B., & Hosni, M. (2016). Characterization of the frequency and nature of bleed air contamination events in commercial aircraft. *Indoor air*, 26(3), 478-488.
- [4] Winder, C. and J. Balouet. 2001. Symptoms of irritation and toxicity in aircrew as a result of exposure to airborne chemicals in aircraft. *Journal of Occupational Health and Safety—Australia and New Zealand*, 17:471–483.
- [5] Murawski, J. T. L. (2011). Case study: Analysis of reported contaminated air events at one major US airline in 2009-10. AIAA, 5089, 2001.
- [6] Nagda NL, Rector HE, Li Zet al. (2001). Determine aircraft supply air contaminants in the engine bleed air supply system on commercial aircraft ENERGEN report numberAS20151, prepared for American society for heating, refrigerating, and air-conditioning engineers, Atlanta, GA. Germantown, MD: ENERGEN Consulting, Inc 20874.
- [7] Guan, J., Gao, K., Wang, C., Yang, X., Lin, C. H., Lu, C., & Gao, P. (2014). Measurements of volatile organic compounds in aircraft cabins. Part I: Methodology and detected VOC species in 107 commercial flights. *Building and Environment*, 72, 154-161.
- [8] Bartl, P., C. Völkl, and M. Kaiser. 2008. Chemical characterization of polyol ester aviation lubricant residues. *Journal of Synthetic Lubrication*, 25(1):1–16.

- [9] Van Netten, C., & Leung, V. (2000). Comparison of the constituents of two jet engine lubricating oils and their volatile pyrolytic degradation products. *Applied occupational and environmental hygiene*, 15(3), 277-283.
- [10] Mann, G. W., Eckels, S. J., & W. Jones, B. (2014). Analysis of particulate size distribution and concentrations from simulated jet engine bleed air incidents. *HVAC&R Research*, 20(7), 780-789.
- [11] Reddall, H. A. (1955). Elimination of engine bleed air contamination (No. 550185). SAE Technical Paper.
- [12] Lebbin, P. (2013). Review of Canadian Flight Deck and Cabin Smoke and Fire Incidents: 2001-2010. *SAE International Journal of Aerospace*, 6(2013-01-2307), 286-298.
- [13] Supplee, D. S., & Murawski, J. T. (2008). An attempt to characterize the frequency, health impact, and operational costs of oil in the cabin and flight deck supply air on US commercial aircraft. *Journal of ASTM International*, 5(5), 1-15.
- [14] Day, G. A. (2015). Aircraft Cabin Bleed Air Contaminants: A Review.
- [15] Winder, C., & Michaelis, S. (2005). Crew effects from toxic exposures on aircraft. In *Air Quality in Airplane Cabins and Similar Enclosed Spaces* (pp. 229-248). Springer Berlin Heidelberg.
- [16] Ross, S. M. (2008). Cognitive function following exposure to contaminated air on commercial aircraft: a case series of 27 pilots seen for clinical purposes. *Journal of Nutritional & Environmental Medicine*, 17(2), 111-126.
- [17] Lambert, E., Johansson, N., (2014, 02/26). Fume events: the current position. Retrieved from <http://www.lexology.com/library/detail.aspx?g=cdfb2845-fa16-48d4-a25d-85f8e4d0b911>.

[18] Roth, J. (2015). *Bleed air oil contamination particulate characterization* (Doctoral dissertation, Kansas State University).

[19] Amiri, S. N., Jones, B., Mohan, K. R., Weisel, C. P., Mann, G., & Roth, J. (2016). Study of Aldehydes, Carbon Monoxide, and Particulate Contaminants Generated in Bleed-Air Simulator. *Journal of Aircraft*, 1-11.

[20] Rice, C. (2003). Validation of approach and climb-out times-in-mode for aircraft emissions computation. *Transportation Research Record: Journal of the Transportation Research Board*, (1850), 79-82.

Appendix A: Project setup pictures



Figure A-1: Engine Test setup during test



Figure A-2: C18 oil injection and sample ports [18]



Figure A-3: Allison Model 250-C18 engine [18]

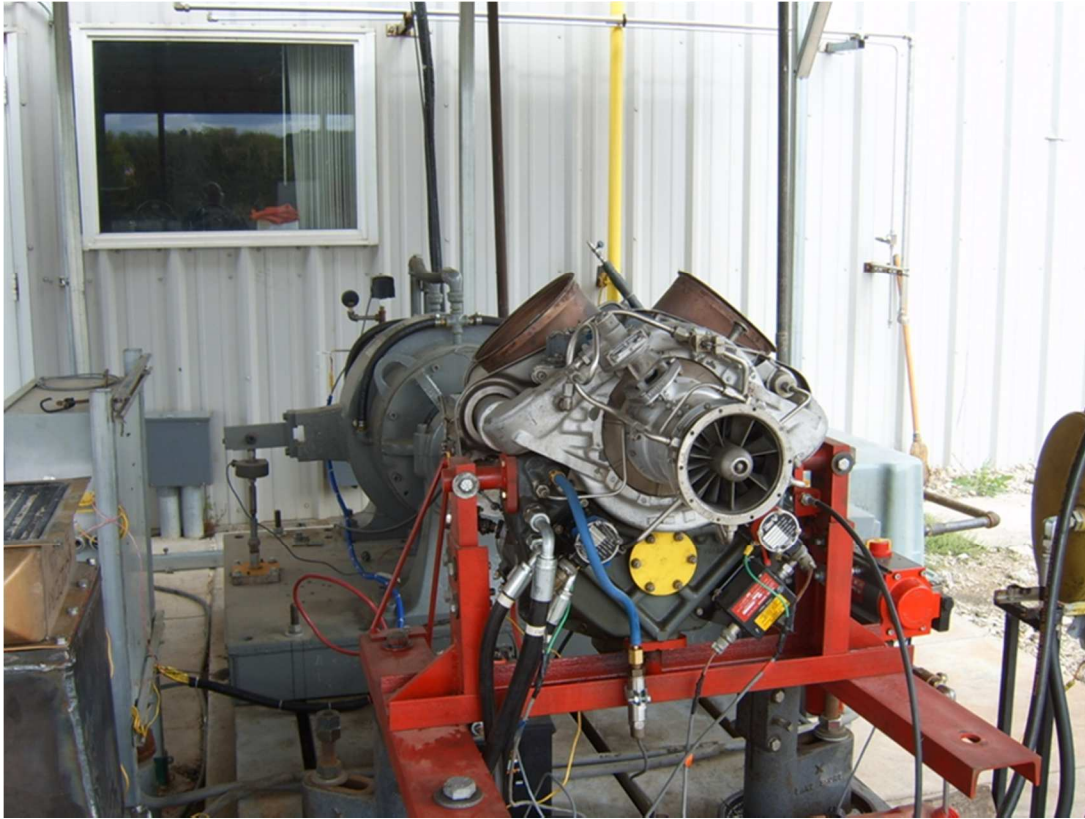


Figure A-3: Allison Model 250-C18 engine during setup



Figure A-4: Allison Model 250-C28B engine [18]



Figure A-5: Allison Model 250-C18 setup



Figure A-6: Allison Model 250-C18 test run

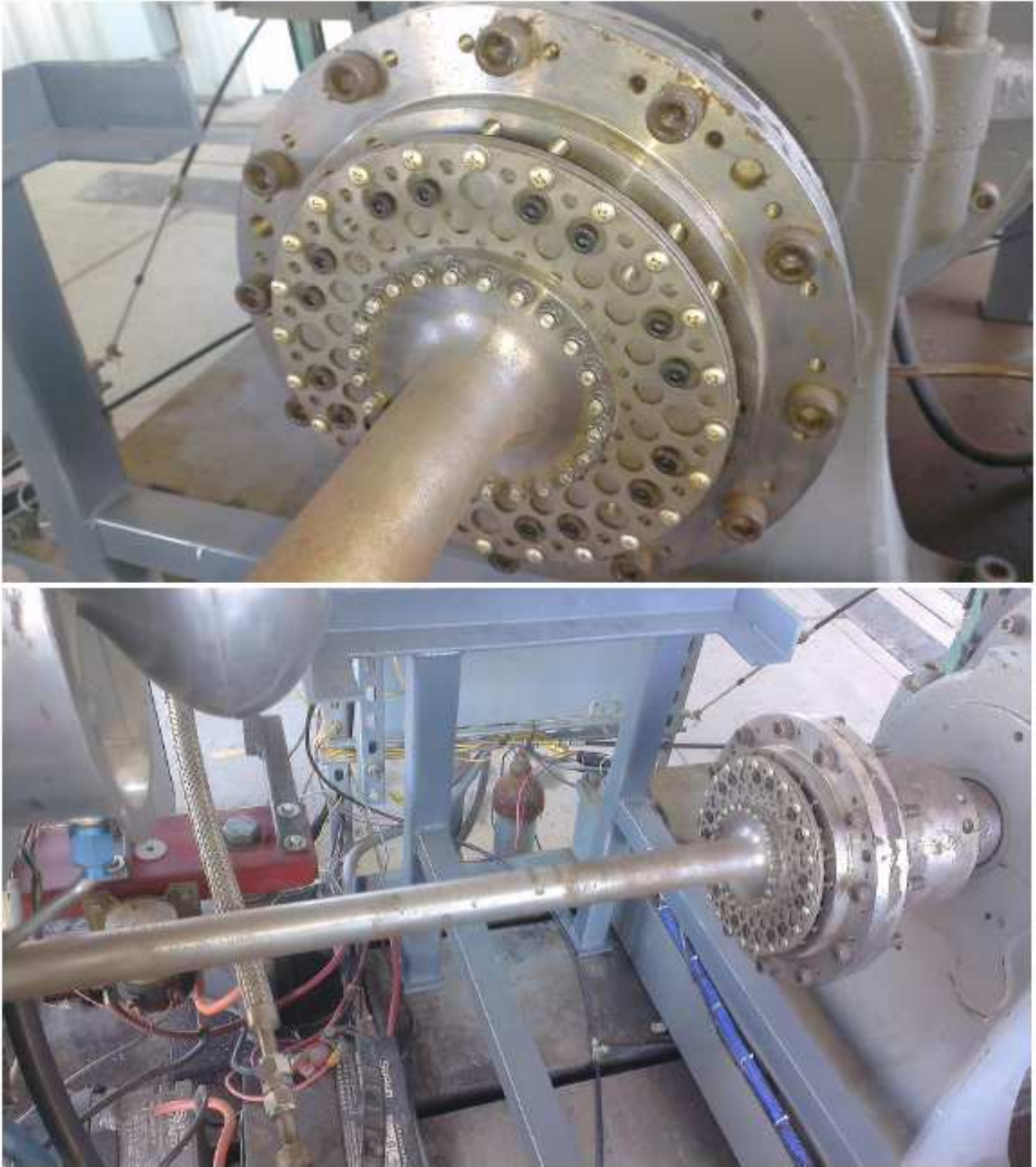


Figure A-7: Driveshaft for engine C18 [18]



Figure A-8: Dynamometer to simulate engine running load



Figure A-9: Allison Model 250-C28B setup



Figure A-10: Allison Model 250-C28B test run